Met.O.770

METEOROLOGICAL OFFICE

Scientific Paper No. 22

The Solution of Atmospheric Diffusion Equations by Electrical Analogue Methods

by J. B. TYLDESLEY, B.A.

LONDON: HER MAJESTY'S STATIONERY OFFICE

PRICE 4*s.* 6*d.* NET

Met.O.770

METEOROLOGICAL OFFICE

Scientific Paper No. 22

The Solution of Atmospheric Diffusion Equations by Electrical Analogue Methods

by J. B. TYLDESLEY, B.A.

LONDON

HER MAJESTY'S STATIONERY OFFICE

1965

U.D.C.: 551·511:
517·9:
681·14

Contents

Summary 1

Introduction 1

The resistance–capacity network 2

The principle of the general-purpose analogue computer 8

Application of computer—continuous line source .. 10

Application of computer—continuous point source .. 19

Application of computer—instantaneous line source .. 30

Application of computer—instantaneous point source 31

Conclusion 34

Choice of analogue or digital methods of computing 34

Acknowledgements 35

Bibliography 35

The Solution of Atmospheric Diffusion Equations by Electrical Analogue Methods

by J. B. Tyldesley, B.A.

SUMMARY

A method of solving the two-dimensional diffusion equation by means of a resistance–capacity network is described, and an application to a continuously emitting infinite cross-wind line source given. This introduction to the basic analogue of diffusion is followed by a description of a more comprehensive computing method using a general-purpose analogue computer.

Methods of obtaining solutions for the continuous line source, continuous point source, and instantaneous line source are given, and some preliminary results are shown. A proposed extension of the method to deal with the instantaneous point source (cluster) is outlined. The variation with height of the parameters is not restricted to simple analytical forms.

INTRODUCTION

For many years it has been customary to treat atmospheric diffusion by representing the turbulent transport of material in a way analogous to heat conduction in a solid. The rate of transport is supposed to be proportional to the gradient of the concentration of the material, and the coefficient of proportionality called 'diffusivity'. This leads to the diffusion equation

$$\frac{\partial \chi}{\partial t}+u\frac{\partial \chi}{\partial x}+v\frac{\partial \chi}{\partial y}+w\frac{\partial \chi}{\partial z} = K_x\frac{\partial^2 \chi}{\partial x^2}+K_y\frac{\partial^2 \chi}{\partial y^2}+\frac{\partial}{\partial z}\left(K_z\frac{\partial \chi}{\partial z}\right)$$

where

x	is distance along the direction of mean horizontal wind
y	is distance across the direction of mean horizontal wind
z	is distance vertically upward
$u,v,w,$	are the wind speeds along the x,y,z axes respectively
K_x,K_y,K_z	are the diffusivities in these directions of the x,y,z axes respectively
t	is time
χ	is the concentration of the material being diffused.

It is assumed that Ks are functions of position only, not of time or of the size of the cloud. Provision is made for K_z to be a function of z, but not for K_x and K_y to vary in the horizontal plane. In addition, it is usually necessary to omit some terms in order to obtain solutions. Along-wind diffusion is usually ignored, and vertical speed put equal to zero. The results of following this line of thought have been summarized by Sutton[1]*, while a notable recent extension was that of Smith[2,3]. The solutions which have been obtained have had only limited success in the prediction of diffusion. In part this is due to the inherent limitations of the diffusivity idea; but the need to use simple forms for the variation of the parameters with height, and to ignore certain terms, also plays a part. It has recently been suspected (Pasquill[4]) that shear of the horizontal wind in combination with vertical

*The index figures refer to the bibliography on page 35.

diffusion, may be an important mechanism for the horizontal spread of diffusing clouds, especially at ranges greater than 20 km. The object of this paper is to put forward methods of obtaining solutions in which the parameters, which include wind shear, may have almost any variation with height. The solutions are numerical, but they are obtained first in terms of dimensionless variables, and may then be applied to various specific cases by suitable choice of units.

In the past few years the Hay–Pasquill* ideas of estimating diffusion by the use of suitably filtered wind fluctuation records have achieved considerable success. However, these statistical theories as they stand are applicable to homogeneous fields of turbulence only, and to overcome this limitation Pasquill[5] has put forward three methods for deriving diffusivities from local fluctuation measurements. One application of the methods to be described is as a computational framework into which such diffusivities, derived from observations, may be put, and concentrations computed as functions of position and time.

The general-purpose analogue computer is a machine designed specifically for the solution of differential equations. Although it has been widely used in the aircraft, electrical engineering and atomic energy fields, there have so far been few applications in meteorology. It is hoped that the present study, apart from its intrinsic interest, will be of use in pointing the way to further openings for analogue techniques in meteorology.

THE RESISTANCE–CAPACITY NETWORK

The diffusion equation for a continuous line source is

$$u\frac{\partial \chi}{\partial x} = \frac{\partial}{\partial z}\left(K\frac{\partial \chi}{\partial z}\right) \qquad \ldots(1)$$

Suppose we have an atmosphere of total depth H, and split it into n layers, each of thickness h, so that $H = nh$. We specify χ and u at the levels n, and K at the intermediate levels $n+\frac{1}{2}$. The usual finite-difference approximation gives

$$u_n\frac{\mathrm{d}\chi_n}{\mathrm{d}x} = \frac{1}{h^2}[K_{n+1/2}(\chi_{n+1}-\chi_n) + K_{n-1/2}(\chi_{n-1}-\chi_n)] \qquad \ldots(2)$$

Now consider the electrical network of Figure 1.

Summing the currents at the node to the right of C_n (at voltage V_n) gives

$$C_n\frac{\mathrm{d}V_n}{\mathrm{d}t} = \left[\frac{1}{R_{n+1/2}}(V_{n+1}-V_n) + \frac{1}{R_{n-1/2}}(V_{n-1}-V_n)\right] \qquad \ldots(3)$$

Comparison with equation (2) shows that an analogue may be established by making

$$V \propto \chi$$

$$t \propto x$$

$$C \propto u$$

$$1/R \propto K$$

Voltage is the dependent variable and time the independent variable. The parameters K and u are set in terms of the components R and C. To start the solution off, the capacitor at the source level is charged to a convenient voltage, all the others being discharged. Thereafter voltage as a function of time corresponds to concentration as a function of distance downwind.

*Advances in Geophysics, London & New York, 6, 1959, p. 345.

Initial condition.—The term 'line source' which is conventionally used, often refers to the convenient mathematical abstraction of an infinitely thin source of infinite concentration. The more practical case of material at finite concentration, initially spread uniformly through a thin layer, will be considered. To simulate this, the capacitor at the source level is charged initially to the maximum working voltage, and all the others are discharged. If a source deeper than one layer is required, adjacent capacitors may be charged. A source of depth less than one layer cannot be represented. In such a case the initial condition is close to the state of affairs some way down-wind of the source.

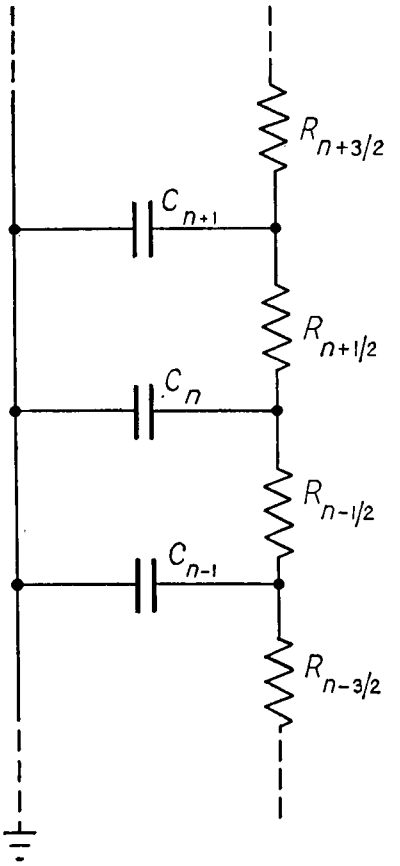

FIGURE 1. The *RC* network.

Boundary conditions.—The lower boundary condition is $K(\partial\chi/\partial z) = 0$, i.e. no flux through the boundary. The analogue may be obtained by the method of images, but it is not necessary to duplicate the chain 'below the ground'. There are two possible arrangements:

(i) Capacitor 'on the boundary' (Figure 2(*a*)).

The equation at node 0 is

$$C_0\frac{dV_0}{dt} = \frac{1}{R_{1/2}}(V_1 - V_0) + \frac{1}{R_{-1/2}}(V_{-1} - V_0)$$

but for no flux,

$$V_1 = V_{-1} \text{ and } R_{1/2} = R_{-1/2}$$

$$\therefore \quad C_0\frac{dV_0}{dt} = \frac{2}{R_{1/2}}(V_1 - V_0).$$

The circuit of Figure 2(*b*) is effectively the same as that of Figure 2(*a*). We halve the capacitor value and omit the 'below ground' part of the circuit. It is incorrect to halve the resistor instead, since its value is already fixed by the equation at node 1.

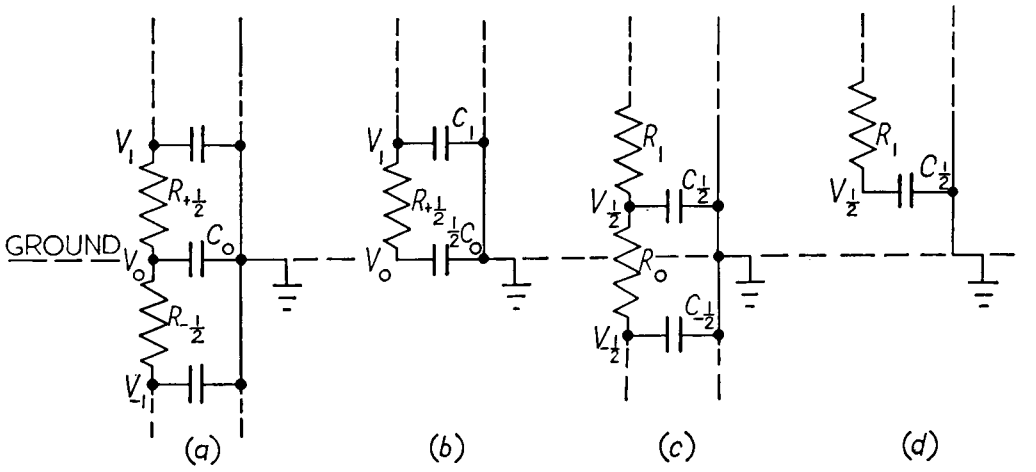

FIGURE 2. Boundary condition for the *RC* network;
(*a*) and (*b*) capacitor 'on the boundary';
(*c*) and (*d*) capacitor 'centred on the layer'.

(ii) Capacitor 'centred on the layer' (Figure 2(*c*)).
The equation at node $\frac{1}{2}$ is

$$C_{1/2}\frac{\mathrm{d}V_{1/2}}{\mathrm{d}t} = \frac{1}{R_{1/2}}(V_{3/2}-V_{1/2})+\frac{1}{R_{-1/2}}(V_{1/2}-V_{-1/2})$$

but

$$V_{1/2} = V_{-1/2}$$

$$\therefore\quad C_{1/2}\frac{\mathrm{d}V_{1/2}}{\mathrm{d}t} = \frac{1}{R_{1/2}}(V_{3/2}-V_{1/2}).$$

All that is necessary to represent this equation is to omit the part of the circuit above node $\frac{1}{2}$ (Figure 2(*d*)). This arrangement is the more straightforward, and is the one used. From this point on, concentrations and wind speeds are specified at the centre of layers, and diffusivities at their boundaries.

The upper boundary condition has to be suited to a finite network, so that $\chi \to 0$ as $z \to \infty$ is not possible. In practice the network is terminated above as well as below, and simulates a reflecting upper boundary. In cases (important in practice) where, because of a marked temperature inversion, such a lid exists in the atmosphere, there is no difficulty. In other cases, the approach is to take the solution only to the point where material begins to appear in the top layer. In these cases the layer spacing must be suitably chosen in relation to the maximum distance downwind for which the solution is desired.

Scaling. Dependent variable.—The 'normalized variable' approach will be used. All voltages may be considered as fractions of the initial voltage on the source capacitor, and all

concentrations as fractions of the concentration in the source layer at $x = 0$. Concentrations and voltages are then each dimensionless numbers with maximum value unity. To transform to absolute units, we make use of the continuity condition

$$Q = \int_0^\infty u\chi \, dz \qquad \ldots(4)$$

where Q is the source strength (i.e. rate of emission per unit length of the cross-wind line). This expresses the fact that the horizontal flux through every vertical plane is equal to the source strength.

Initially $Q = u_s\chi_s h$ (the subscript s refers to source)

$$\text{and } \chi_s = Q/u_s h.$$

The value on the concentration scale, labelled 1 in normalized units, is relabelled $Q/u_s h$. Alternatively, the label 1 may be left, but the quantity referred to entered as $(u_s h/Q)\,\chi$. It is a matter of convenience which method is adopted.

Independent variable.—It was mentioned above that time in the model (τ) represents distance downwind in the atmosphere (x). Put

$$\tau = \beta x \qquad \ldots(5)$$

On substituting (5) in (2) and comparing with (3) we find that for the analogy to hold

$$\frac{\beta}{CR} = \frac{K}{uh^2} \quad \text{and} \quad \beta = \frac{K}{uh^2}CR \qquad \ldots(6)$$

for all points of the network. CR will be recognized as having the dimension time. Once the CR values are decided, the equations (5) and (6) can be used to relabel the recorder time axis (τ) in terms of downwind distance x. β must be the same at all levels.

Next we consider the relation between the CR values and the solution time. Consider a layer of depth $H = nh$, with K and u constant. The classical expression for the standard deviation σ of the vertical distribution of material dispersion due to diffusion is $\sigma^2 = 2Kt$. If little material is to reach the top of the layer, $\sigma^2 = H^2/10$ (say) at the end of the computation. Then if x_m is the approximate distance at which the standard deviation reaches this value we have

$$\frac{H^2}{10} = \frac{n^2h^2}{10} = 2K\frac{x_m}{u}$$

$$\text{i.e. } x_m = \frac{n^2h^2u}{20K} \qquad \ldots(7)$$

Equation (7) shows, for given K and u, what distance of travel to take. Eliminating u/K by means of the time-scale factor (6)

$$\tau_m = \frac{n^2}{20}CR \qquad \ldots(8)$$

This equation shows that, as to order of magnitude, the solution time depends on the number of layers and the circuit time-constant, but not on the parameter values. This important result, which may be thought almost obvious in this case, will be of use when the scaling of the general-purpose analogue computer is considered.

Constructing the analogue.—The object was to construct the analogue from readily available components, in order to get an idea of the results that might be expected from more refined equipment. Bearing in mind the approximate nature of our knowledge of the variation of K, high accuracy was not aimed at. The recorders available were pen milliammeters, with a frequency response of only 1 c/s or so. This indicated a solution time of the order of tens of seconds. It is desirable to use as many layers as possible in order to minimize finite-difference errors. On the other hand, the charge initially on the source capacitor is eventually distributed among all the capacitors of the chain, so that with many capacitors the voltages at the end of the solution occupy only a small part of the recorder full scale. Balancing these opposed considerations, it was decided to use ten capacitors. Putting $n = 10$ in (8) we get $\tau_m = 5CR$. The sort of solution time dictated by the recorder requires CR to be in the range 1–10 seconds. The largest good-quality capacitors available were 2μF, which with resistors of 5MΩ would give a CR value of 10 seconds. The largest resistance available was 10MΩ, so that it was possible to attain the necessary time constants without trouble. But it was clear that there would be difficulty in ensuring that, in the process of recording the voltage distribution in the network, the distribution itself was not disturbed. To draw no appreciable current from the computing chain, the recorder must have a resistance large compared with the resistances of the chain, say 1000MΩ. The resistance of the recorders was 3000Ω, while even that of a commercial valve-voltmeter is only 10–100MΩ. This difficulty, of making a good pen recording of the output voltages of a network analogue, is not much touched upon in publications on the subject. Use was made of a d.c. amplifier, developed for another purpose[6] in which the input goes direct to the grid of a pentode, and which has a low-impedance cathode-follower output. This was modified slightly for single-ended operation and inserted as a buffer between the computing chain and the pen recorder. The amplifier showed a small non-linearity, about one per cent of full scale. This, negligible for the purpose for which it was designed, was significant in this application because in large parts of the solutions, deflections were around one tenth of full scale. Some drift due to grid-current charging of the input valve, was noticed also.

Some difficulty was experienced at first in discharging all the capacitors simultaneously while they were interconnected through the resistors, and in charging the source capacitor to the full initial value. The circuit of Figure 3 which is repeated at each capacitor, was designed to overcome this. Initially the switch is in position 1. A jack-plug carries the source voltage (one volt) derived from a dry battery, and is inserted in the socket S_1 of the capacitor

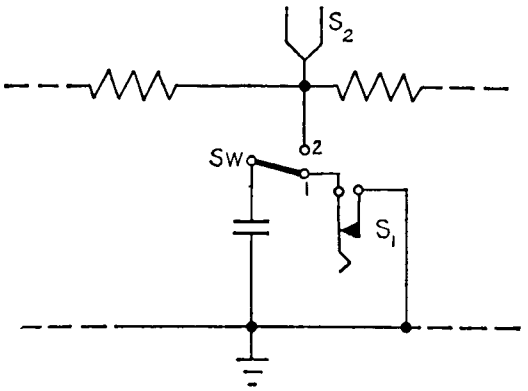

FIGURE 3. Initial condition arrangement for the RC network.

corresponding to the source level. This capacitor is charged to the source voltage, but all the others are shorted to earth through the normally-closed contacts of the jack-sockets. To start the computation, the switch (which is a ten-pole two-way wafer) is turned to position 2. Thus all the capacitors are simultaneously disconnected from earth (or voltage source) and connected to the appropriate places in the resistor chain. Another socket S_2 to each capacitor allows selection of the voltage to be recorded.

The oil-filled paper-dielectric capacitors used were $2\mu F \pm 10$ per cent. The resistors were ± 5 per cent composition types, and could be changed by insertion into screw-up junction strips. The capacitors, junction strips, switch, sockets and battery for voltage source were mounted on a base-board. The amplifier and recorder had three channels, each of which could be plugged to any of the ten capacitors. Figure 4 shows the complete assembly.

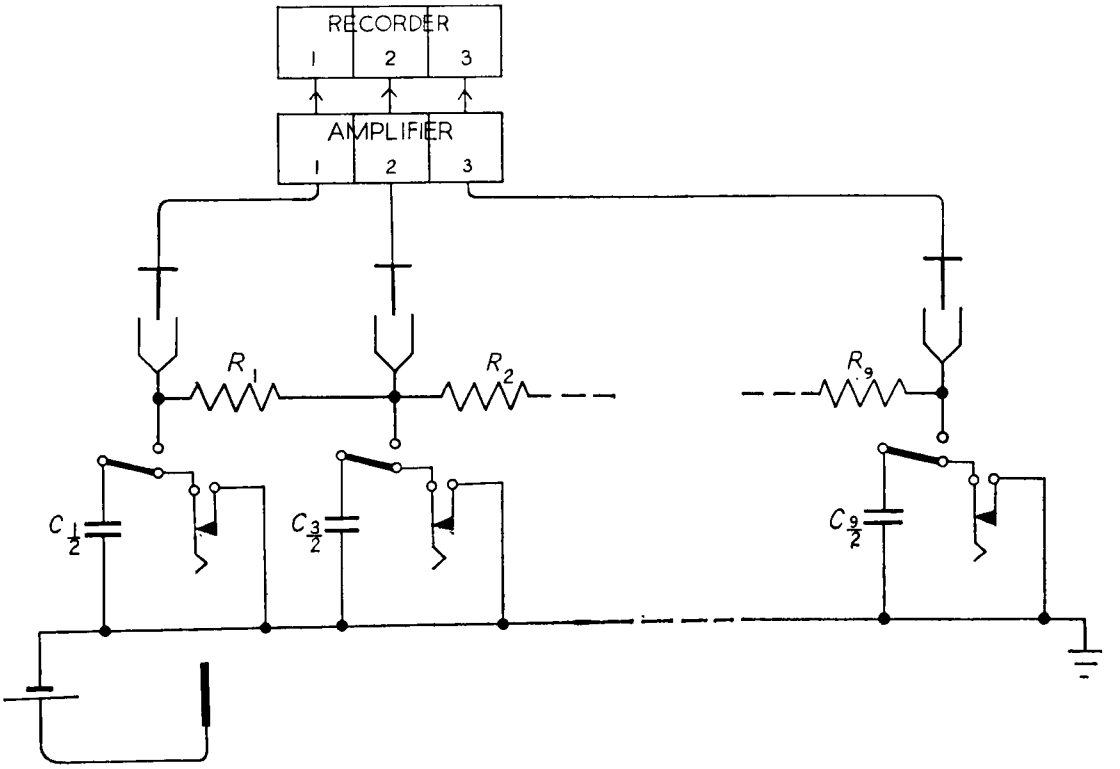

FIGURE 4. The complete *RC* network assembly.

Solutions were obtained for a number of variations with height of the parameters u and K, including u and K constant; and u constant, K decreasing linearly with height. The relations for the peak ground-level concentrations (χ_m) from an elevated line-source, and the distance downwind (x_m) at which it occurs, for u and K constant, were also obtained, and compared with the theoretical $\chi_m \propto 1/a$, $x_m \propto 1/a^2$ (height of source a). In general the solutions obtained were in fair agreement with theory, although some smoothing had to be applied to the concentration isopleths. An interesting use was made of the apparatus by N. Thompson, and has been described in detail elsewhere[7], but briefly values of K were

derived from turbulence statistics and combined with observed values of u to compute vertical concentration profiles at a range of 100m. These were then compared with observed concentration profiles. The K values were derived for a number of values of the Lagrangian/Eulerian scale-ratio, and the effective value of this ratio taken as that which gave the computed profile best in agreement with observation. The difficulty of the fixed capacitors was overcome by using a special large capacitor at the bottom layer, and making use of the ± 10 per cent deviation from the nominal values above this. The experiments were carried out in stable conditions, in which most of the variation of wind with height is near the ground, and therefore it was possible to obtain a tolerable fit to the observed profiles.

No detailed results using the RC network will be given, because the work done with it was later repeated with improved accuracy using the general-purpose computer. The disadvantages of the network were:

(i) Difficulty of changing parameters
(ii) Amplifier drift
(iii) Amplifier and recorder non-linearity.

Moreover the method could not easily be extended to an increased number of dimensions. The following sections will show how the general-purpose machine overcomes these difficulties. The time devoted to the network analogue was nevertheless well spent. It enabled us to get a grasp of the essentials of electrical analogue work, using cheap and easily obtainable apparatus. It also suggested a method of scaling specially appropriate to our work, differing radically from that advocated by the manufacturer of the general-purpose machine.

THE PRINCIPLE OF THE GENERAL-PURPOSE ANALOGUE COMPUTER

This section can give only a highly-compressed sketch of a subject on which substantial books have been written, and the reader interested in a fuller and more rigorous treatment is referred to them (e.g. Karplus and Soroka[8], Jackson[9]).

The type of machine to be described has one independent variable, time; and may have any number of dependent variables, voltages. Anyone who attempts to write down circuits to perform arithmetic operations soon finds that the crux of the problem is *loading*—that is, the disturbance of the functioning of one part of a circuit by the adjacent parts which perform subsequent operations. A buffer between sections is therefore required, drawing no current from the preceding section, but supplying as much as may be required to subsequent sections. The modern d.c. amplifier, known in this context as an 'operational amplifier', provides this. Its high gain is used not primarily for voltage amplification, but to ensure good linearity. Its high input impedance and low output impedance give the necessary buffer action, and its low drift enables it to be used to form a stable integrator. In use, passive elements are added to the amplifier, to give units for summing and integrating. Potentiometers (simple resistive attenuators) are used to multiply by constants in the range 0–1. The conventional symbols for the units, and their functions are given in Figure 5. As well as the input and output connexions shown, all amplifiers have a common earth connexion. It is useful to remember that the triangular symbols point from input to output.

The inputs to summer and integrator are not limited to three. It will be noticed that in each case there is a change of sign between input and output. When subtraction is to be carried out, one tries to arrange for the quantities to be available with opposite sign at the

input of a summer. Where this is not possible, one input may be inverted first, using a summer with a single input. Arrangements are made to impose any desired initial conditions on the integrators, before the computation begins. A stable voltage supply, at the maximum working voltage of the amplifiers (typically ± 100v) is provided. The initial conditions on integrators are derived from it; and it is also used, in conjunction with a digital voltmeter, in setting the potentiometers.

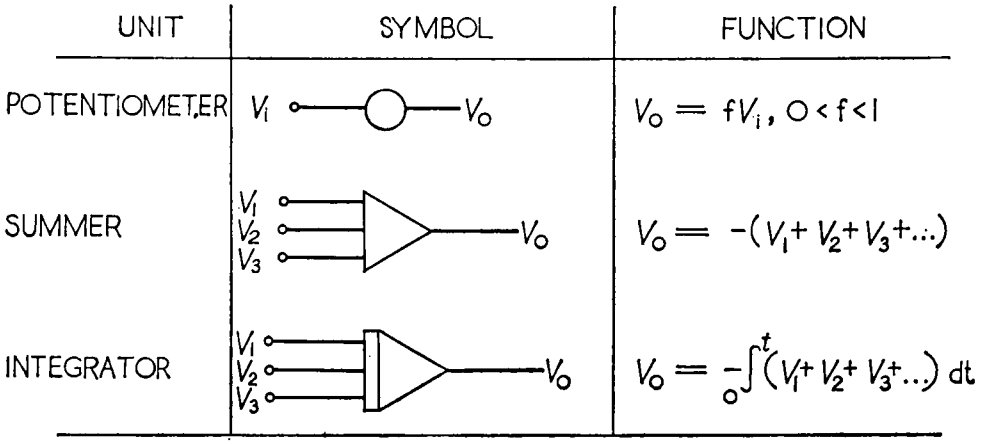

FIGURE 5. Computer units—symbols and functions.

To solve differential equations, the computing units are connected in closed feed-back loops. Imagine for the moment that a voltage proportional to the highest order derivative is available. By applying it to an integrator, the next lower derivative is obtained. Then by applying this output to another integrator, and so on, all the derivatives, and finally the dependent variable itself, will be obtained. The voltage proportional to the highest derivative is formed according to the differential equation. Rewriting the equation with the highest derivative on the left-hand side, and all other terms on the right, will show in every case how the integrator outputs must be combined to obtain the correct feed-back to the start of the integrator chain. The procedure for dealing with simultaneous equations is similar. A separate integrator chain is set up for each dependent variable; these are interconnected as necessary. The two-dimensional diffusion problem will be used as an example in the next section.

A word should be said on the practical arrangement of the computer. The work to be described was done on the PACE 231R computer at the Royal Armament Research and Development Establishment, Fort Halstead, on which the arrangements are typical of modern commercial analogue machines. The equipment is housed in cabinets, and all connexions are brought to a central plug-board, or 'patch-panel'. The units are interconnected in the desired way by plugging screened leads into the panel, which can be removed bodily with its leads and preserved for later use. The potentiometers controlling the initial conditions and parameter values are set manually, using a built-in digital voltmeter. The initial conditions are applied to the integrators by relays. Output voltages may be read on the digital voltmeter, or recorded on an eight-channel pen-recorder, or on a two-co-ordinate plotter. The plotter, which uses paper 25×35 cm, was used for most of this work. When time is required as one co-ordinate, that channel is connected to an integrator fed from a constant voltage.

The solution time is chosen to be long enough to avoid high-frequency errors, but not so long as to make integrator drift a problem. With times of 10–100 seconds, no difficulties arise on either score when using PACE. It will be noted that a complex problem requires no longer to run than a simple one, but merely more equipment. This is in marked contrast to the situation in digital computing, whether by hand or automatic. It means that the analogue machine can handle expeditiously problems, however large, up to the limit of its available machine units. Beyond that capacity, it can do nothing. The number of linear units in the Fort Halstead machine is given below:

Unit	*Number available*
Amplifier, summer or integrator	30
Amplifier, summer only	45
Potentiometers, manual	100

APPLICATION OF COMPUTER—CONTINUOUS LINE SOURCE

In attempting to solve partial differential equations, the central problem is that the analogue computer has only one independent variable, time. Therefore finite differences are taken in the other independent variable, and a set of ordinary simultaneous differential equations is obtained. In choosing which independent variable shall be continuous and which represented by finite differences, both economy of equipment in setting up the resulting equations, and ease of introduction of the boundary conditions is considered. For the two-dimensional diffusion problem, it proves to be most convenient to take downwind distance x as the continuous variable. Only one integration has to be performed, the coefficients u and K are constant with x; and the no-flux boundary condition is dealt with by terminating the computing chain, just as in the network analogue. The equation in finite-difference form is again

$$u_0\frac{d\chi_0}{dx} = \frac{1}{h^2}[K_{1/2}(\chi_1-\chi_0)+K_{-1/2}(\chi_{-1}-\chi_0)]$$

where the ns have been dropped for convenience. This may be rewritten as

$$\frac{d\chi_0}{dx} = a_0\chi_{-1}-b_0\chi_0+c_0\chi_{-1} \qquad \ldots(10)$$

where

$$a_0 = \frac{K_{-1/2}}{u_0h^2} \qquad b_0 = \frac{K_{1/2}+K_{-1/2}}{u_0h^2} \qquad c_0 = \frac{K_{1/2}}{u_0h^2}$$

which may be set up on the machine with great economy using one integrator and three potentiometers per layer, and no other amplifiers. Such a circuit was used by Brock[10]. It had earlier been used for heat-conduction problems (Jackson[9] p. 310). Although simple to set up, this circuit is not the easiest to use when many runs have to be made with different sets of parameters. Altering one parameter changes several coefficients, which have to be worked out by hand before they can be set up on the computer. A circuit was therefore devised, in which each potentiometer corresponds to one parameter at one level. This proved a great convenience, especially when it was desired to run a series of values of K

without changing the values of u. Part of this circuit is given in Figure 6. In all, ten layers were used. The alternate signs for the χs are retained, and it will be seen that there is still only one integrator per layer. The Ks and us are entirely independent, but the latter is set as $1/u$. As a result zero values of u must be avoided, but this raises no difficulty in practice.

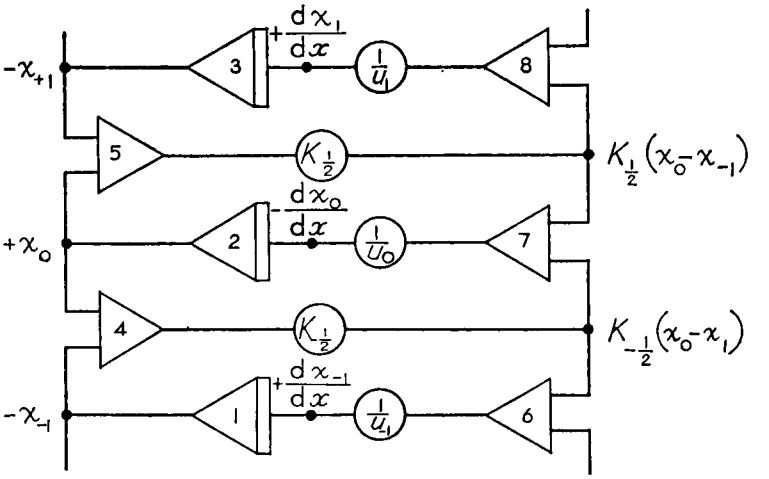

FIGURE 6. Two-dimensional diffusion—computer diagram.

In scaling the problem, interest centres on the parameters rather than the variables. Since the potentiometer is an attenuator, with input a voltage and output a smaller voltage, the attenuation factor (or potentiometer setting) is a dimensionless number in the range 0–1. It seems natural to form such a number by normalizing the parameters relative to their maximum values. The maximum value used may be, not the strict maximum of the problem, but some rather larger but more convenient value. It may not be smaller, however, since the resulting potentiometer setting would be greater than unity. Dashed values will be used throughout for computer values of parameters and variables, and suffix m for maximum (or reference) values. So we write

$$K' = \frac{K}{K_m} \qquad \left(\frac{1}{u}\right)' = \frac{(1/u)}{(1/u)_m}$$

Note that

$$\left(\frac{1}{u}\right)_{\max} = \frac{1}{u_{\min}} \neq \frac{1}{u_{\max}}.$$

The reference value of u is therefore the *smallest* value.

Referring to Figure 6 the action of the computer can be followed. The initial condition is that one integrator output gives full computer reference of unity (source layer) while all the others give zero. The maximum input to the summers 4 and 5 is also 1. They are therefore operated on a gain of 1, with potentiometers on the output set to $K' = K/K_m$, giving outputs of $K'_{+1/2}\ (\chi_1 - \chi_0)$ and $K'_{-1/2}\ (\chi_{-1} - \chi_0)$ respectively. These outputs are summed in amplifier 7, also on a gain of 1, giving

$$-\frac{1}{K_m}[K_{1/2}(\chi_1 - \chi_0) + K_{-1/2}(\chi_{-1} - \chi_0)]$$

Amplifier 7 is followed by a potentiometer set to $(1/u)' = (1/u)/(1/u)_m$. The input to integrator 2 is therefore

$$-\frac{(1/u)_0}{K_m(1/u)_m}[K_{1/2}(\chi_1-\chi_0)+K_{-1/2}(\chi_{-1}-\chi_0)]$$

and the integrator output is

$$\frac{(1/u)_0}{K_m(1/u)_m}\cdot\frac{1}{CR}\int[K_{1/2}(\chi_1-\chi_0)+K_{-1/2}(\chi_{-1}-\chi_0)]\,d\tau$$

If we substitute the time-scale factor given by $\tau = \beta x$ in the above, and compare with (2) we find

$$\beta = \frac{K_m(1/u)_m CR}{h^2}. \qquad \ldots(11)$$

This shows how to relabel the τ-axis of a recording in terms of x:

$$x = \frac{\tau}{\beta} = \frac{\tau}{CR}\cdot\frac{h^2}{K_m(1/u)_m}.$$

In all this work, the value of CR was 1 second, so it will frequently be dropped from equation (11). Its presence must, of course, not be ignored when checking the dimensions of equations.

Finally, the concentration axis is relabelled in exactly the same way as with the network analogue, the computer value 1 taking the value Q/u_0h.

As before, instead of relabelling each point on the axes, it may be more convenient to leave the labels as they are, taking them to refer to the dimensionless variables

$$\frac{\tau}{CR} = \frac{K_m(1/u)_m}{h^2}x \quad \text{(independent variable)}$$

and computer reference $\chi' = 1 = (u_0h/Q)\chi$ (dependent variable).

The dimensionless variable in the z-direction is z/H, where H is the total thickness of the layers. Since there are ten layers, it is related to the layer number n by

$$\frac{z}{H} = \frac{n}{10}$$

Figure 7 shows a computer recording for K and u constant with height, and source in the bottom layer. The initial rapid drop in concentration in the source layer is not shown, in order to have an expanded scale in the later part of the solution, but it can of course be recorded if required. Certain features of the solution will be noticed. Going upwards (n increasing) the concentration goes through a maximum at a progressively greater distance downwind. The maxima become flatter, and disappear above the fifth layer. The concentrations in the sixth and higher layers rise monotonically towards a value corresponding to complete mixing through the whole depth H. This concentration is 1/10 of the initial value, as expected for ten layers.

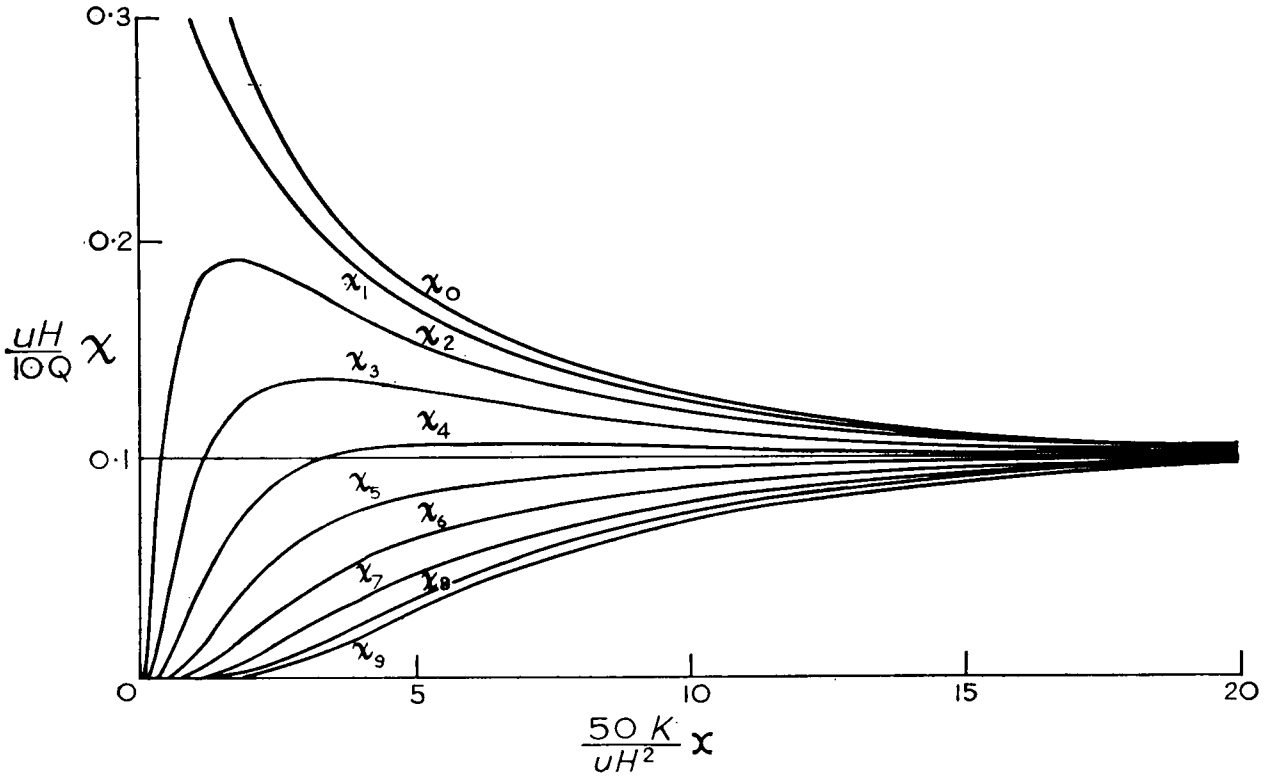

FIGURE 7. Continuous line source—computer recording for u = const., K = const. Source in bottom layer ($n = \frac{1}{2}$).

By reading concentrations off the graph and plotting them on an x–z diagram, vertical sections of the distribution may be constructed. Figure 8 shows such a section for the case u = constant, $K = K_0(H-z)$. Since K decreases to zero at the top of the layer, the no-flux boundary condition at the top is appropriate. This section has been compared with a section by F. B. Smith, based on his series solution for this case. (Unpublished government report). The agreement is remarkably good, although it must be mentioned that the horizontal scale is such that no detailed comparison can be made near the source.

Estimation of Errors.—Errors will arise in the computations due to

(i) Source assumption.
(ii) Finite-difference approximation.
(iii) Upper boundary condition (if this boundary imposed by the apparatus is not high enough to simulate the real diffusion depth).
(iv) Computer error (drift, non-linearity, plotting error).

To form an idea of the importance of these, the computer solutions for K = constant, u = constant and an impervious upper boundary, were compared with the known analytical solution for an atmosphere unbounded above:

$$\chi = \frac{Q}{\sqrt{\pi Kux}} \exp\left[-\frac{uz^2}{4Kx}\right] \qquad \ldots(12)$$

Introducing the dimensionless variables

$$x' = \frac{K}{uH^2}x \qquad z' = \frac{z}{H} \qquad \chi' = \frac{uH}{Q}\chi$$

(12) becomes

$$\chi' = \frac{1}{\sqrt{\pi x'}}\exp\left[-\frac{z'^2}{4x'}\right]$$

and this may be used to calculate values of χ' directly comparable with those obtained

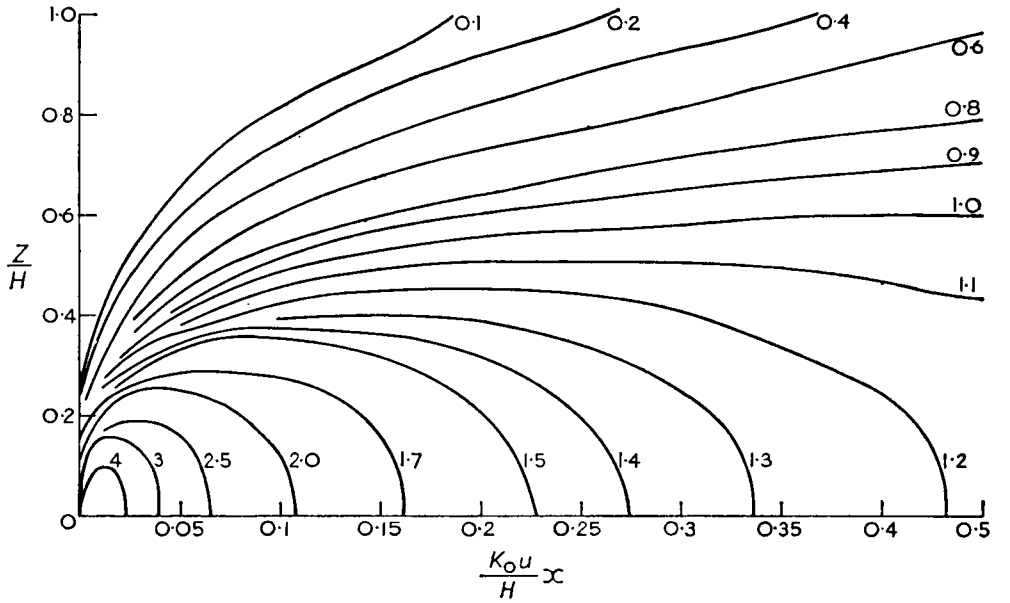

FIGURE 8. Continuous line source—concentrations in XZ plane in units of Q/uH for u = const., $K = K_0(H-z)$.

from the computer. This is done in Figures 9–13. In each case a logarithmic scale is used for x, to give an expanded scale in the rapidly-varying part of the solution, and to allow a detailed examination of the critical region near the source. The graphs are in fact composites, assembled from a number of computations, each designed to give the best possible resolution in some area of the solution. Figure 9 shows the computed concentrations. Figure 10 shows the deviations of the computed from the analytical values in absolute units, while Figure 11 shows the deviations as a percentage of the theoretical values. Different applications will make one or the other approach more appropriate. Sometimes it will be desired to know by what factor a computed value may be in error, but often a large percentage error will be unimportant if the concentration itself is low enough. Figure 10 shows that there is an area near the source where the computed concentration is too small near the ground, and too large above. This is to be expected from the nature of the source assumption. As soon as the cloud meets the upper boundary, deviations appear

there, and propagate steadily downward. Between these two regions, there is a large area of good agreement, with errors 3 per cent or less (Figure 11). The ground concentration agrees to within 3 per cent from $x' = 0{\cdot}005$ to $x' = 0{\cdot}25$, a range of 50:1. This is ample for practical purposes of prediction. Moreover, the upper restriction on x is a result of the upper boundary assumption, and where this assumption is valid, the restriction will not occur. Figure 11 shows another region of high percentage errors near the upper boundary of the cloud, but the low absolute errors in the same region of Figure 10 indicate that the high percentage errors in Figure 11 are in a region of low concentration and therefore will seldom be significant.

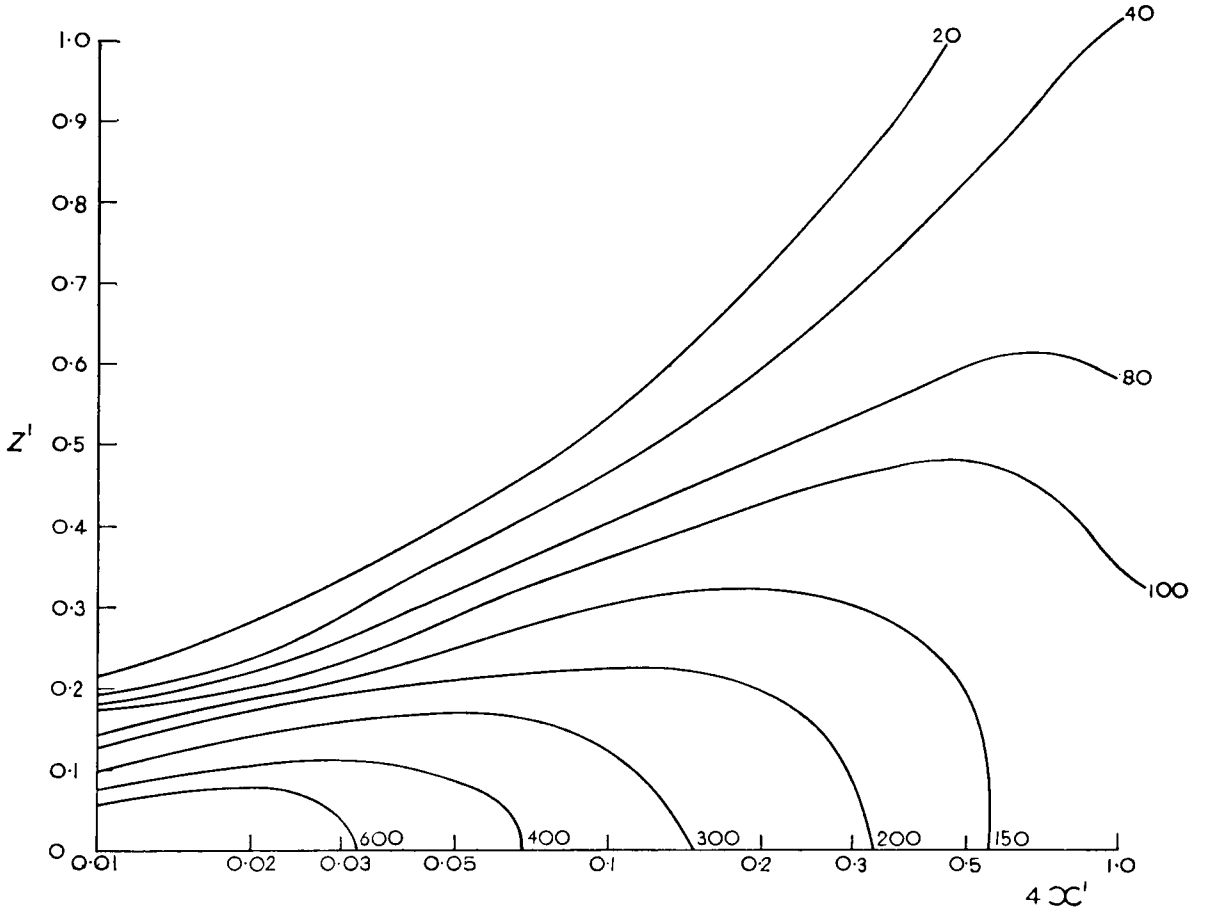

FIGURE 9. Continuous line source—computed concentrations in units of $Q/100uH$ for u = const., K = const.

It was mentioned above that the source assumption, with the material spread uniformly through the source layer, represents more nearly the state of affairs a little way downwind of the source, than that at the source itself. It seemed possible that moving the origin of x' a little way to the left might decrease the source errors. A suitable shift of origin was chosen empirically, to minimize the errors at the bottom layer near the start of the solution. Figures 12 and 13 show that the improvement was outweighed by increased errors elsewhere, and it was concluded that the proper course is merely to ignore the solution near the source. This does not mean that this part of the solution cannot be found. It can always

be computed separately by adopting a smaller layer-spacing. The only proviso is, that whether the model atmosphere in question is bounded above or not, the subsidiary solution must not be taken to the point where the upper boundary begins to have effect.

These results, strictly applicable only to the case for which they were obtained, should form a useful guide to the order of magnitude of errors in other cases. In particular, it appears that away from the regions where the sources of error (i) and (iii) are significant, the combined effects of (ii) and (iv) are less than 3 per cent.

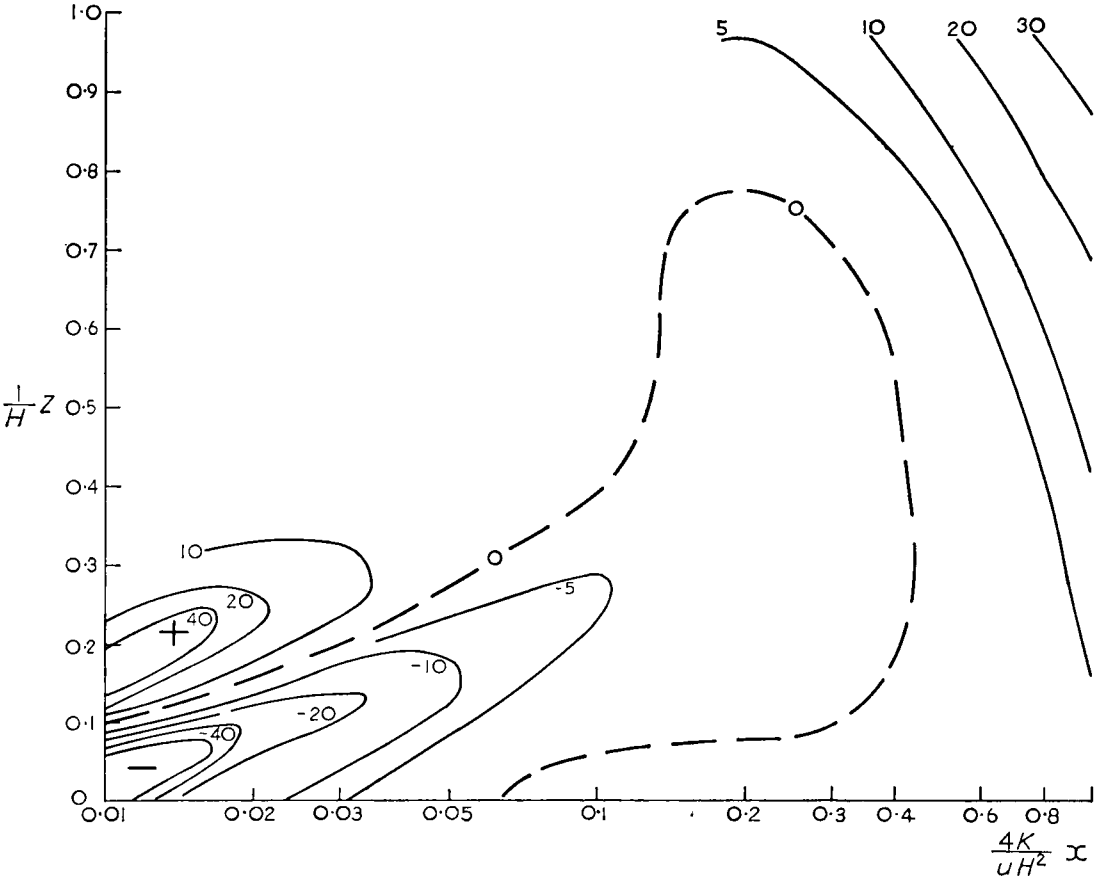

FIGURE 10. Continuous line source—computed concentrations minus theoretical concentrations in units of $Q/100uH$, for u = const., K = const.

Although the machine has thirty integrators, there are a number of practical reasons for not increasing the number of layers. First, an increased number of potentiometer settings has to be worked out, and the values set by hand for each computation. Second, the solution time increases as the square of the number of layers (see Equation (8)), and as the solutions at the various levels are recorded one by one on the two-co-ordinate plotter, the total recording time increases as the cube of the number of layers. A final point is most easily appreciated in the case of the *RC* network, but applies equally to the general-purpose

machine. The charge, initially on the source capacitor, is ultimately divided among all the layers. The final voltage is the initial voltage divided by the number of layers, and the more layers there are, the poorer is the discrimination of the later stages of the solution. The conclusion is that the best number of layers to use is not the maximum possible but the minimum compatible with useful accuracy. As it has been shown that ten layers give errors not exceeding 3 per cent over the part of the solution of interest, it is clear that this number is ample for practical purposes.

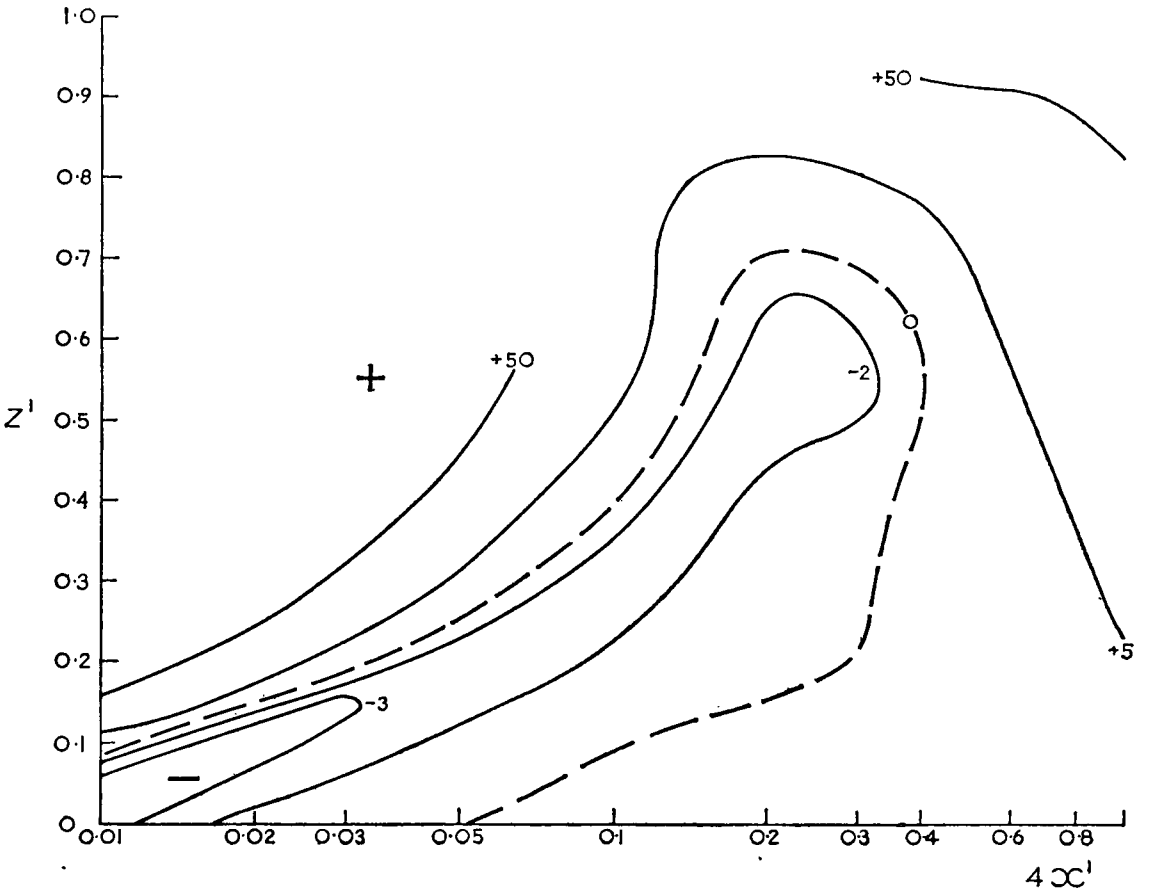

FIGURE 11. Continuous line source—computed concentrations minus analytical concentrations as a percentage of the analytical values, for u = const., K = const.

The largest amount of computation for the two-dimensional case has been on the aniline diffusion experiments mentioned earlier (p. 7). This work will not be described in detail here, but Figures 14 (*a*) and (*b*) show an observed aniline profile, together with profiles computed by the *RC* network (*b*), and by the general-purpose computer, (*a*). One hundred and forty separate runs on the general-purpose machine have been made for this work.

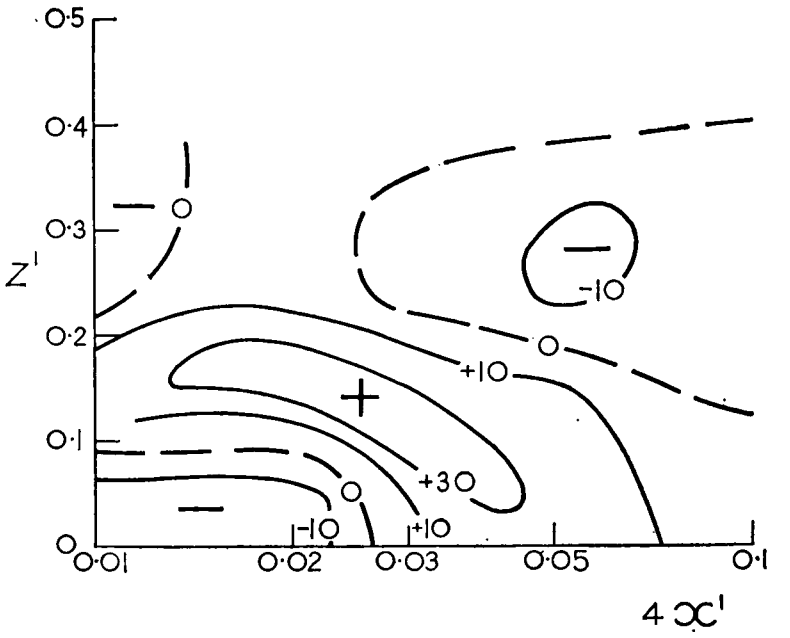

FIGURE 12. Continuous line source—computed concentrations minus theoretical concentrations in units of $Q/100uH$ for u = const., K = const. (As Figure 10, but origin of computed concentrations moved upwind by $x' = Kx/uH^2 = 0{\cdot}001$).

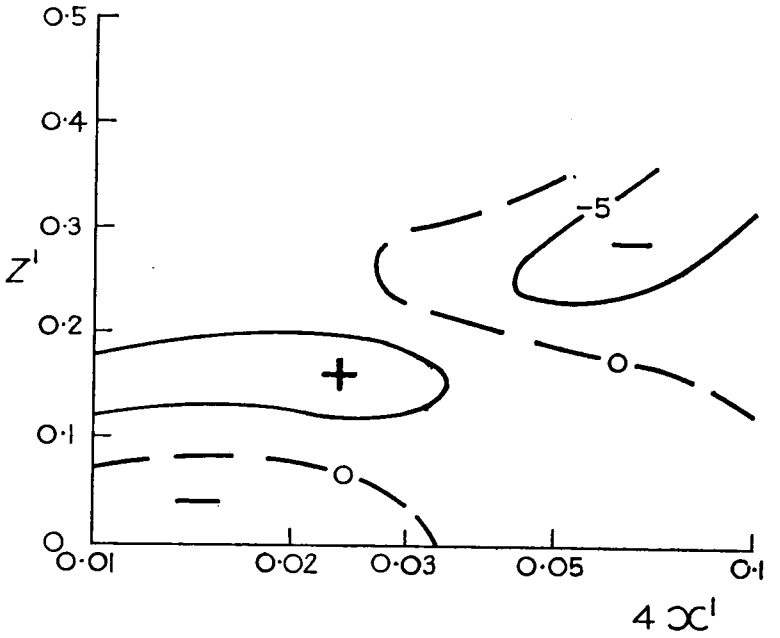

FIGURE 13. Continuous line source—computed concentrations minus analytical concentrations as a percentage of the analytical values, for u = const., K = const. (As Figure 11, but origin of computed concentrations moved upwind by $x' = Kx/uH^2 = 0{\cdot}001$).

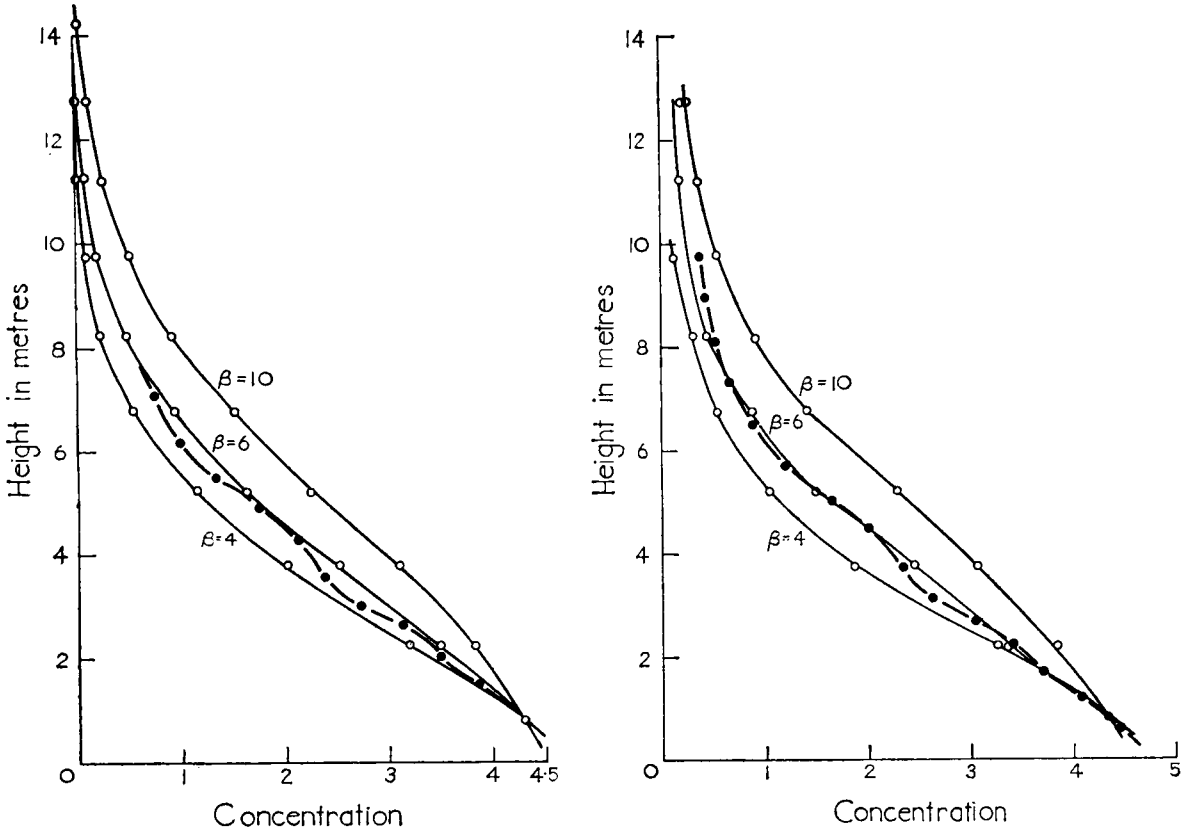

(a) Computed concentrations by general-purpose analogue computer

(*b*) Computed concentrations by *RC* network

FIGURE 14. Continuous line source—comparison of observed and computed diffusion under stable conditions, at range 100 m.
o—o computed concentrations, —·—·— observed concentrations. The β values are the ratio of the Lagrangian and Eulerian scales. The concentrations are in arbitrary units and are made to coincide at 0·75 m.

APPLICATION OF COMPUTER—CONTINUOUS POINT SOURCE

The equation in this case is

$$u\frac{\partial \chi}{\partial x} + v\frac{\partial \chi}{\partial y} = \frac{\partial}{\partial z}\left(K_z \frac{\partial \chi}{\partial z}\right) + K_y \frac{\partial^2 \chi}{\partial y^2} \qquad \ldots (13)$$

with the continuity condition

$$\int_0^\infty \int_{-\infty}^\infty u\chi \, dy \, dz = Q \qquad \ldots (14)$$

where Q is now the amount of material emitted per unit time.

As in the two-dimensional case, conservation of matter is ensured by the impervious upper and lower boundaries, and no additional instrumentation is necessary to deal with equation (14). It is merely used to find the proper scaling relation for the concentrations.

The standard approach to equation (13) would be to take finite differences in the extra dimension y, as well as in z, but this would require a very large amount of computing equipment. For instance, ten layers in y as well as ten in z would require 100 integrators, and corresponding numbers of summers and potentiometers. This is well beyond the capacity of any machine accessible to us. Recognizing that the cross-wind distributions will be of single-humped type, a computation is made at each level of z of the first three moments of the cross-wind distribution defined by

$$C_n = \int_{-\infty}^{\infty} \chi y^n \, dy \qquad n = 0, 1, 2 \qquad \ldots (15)$$

The zero-order moment gives the total amount of material in each layer. The displacements of the centroids of the material are given by

$$Y = \frac{C_1}{C_0} \qquad \ldots (16)$$

and the standard deviations by

$$\sigma^2 = \frac{C_2}{C_0} - \left(\frac{C_1}{C_0}\right)^2 \qquad \ldots (17)$$

In principle, higher moments could be computed and thus the skewness and kurtosis of the distributions found. From a practical point of view, it is very seldom that sampling in the atmosphere can be carried out with an accuracy that makes it possible to say whether the cross-wind distribution is Gaussian or not. It is sufficient therefore to use the first three moments, the differential equations for which are formed by multiplying (13) by the appropriate power of y, integrating, and applying the definitions (15).

They are

$$u\frac{\partial C_0}{\partial x} = \frac{\partial}{\partial z}\left(K_z \frac{\partial C_0}{\partial z}\right) \qquad \ldots (18)$$

$$u\frac{\partial C_1}{\partial x} = \frac{\partial}{\partial z}\left(K_z \frac{\partial C_1}{\partial z}\right) + vC_0 \qquad \ldots (19)$$

$$u\frac{\partial C_2}{\partial x} = \frac{\partial}{\partial z}\left(K_z \frac{\partial C_2}{\partial z}\right) + 2vC_1 + 2K_yC_0 \qquad \ldots (20)$$

The continuity equation (14) becomes

$$\int_0^{\infty} uC_0 \, dz = Q \qquad \ldots (21)$$

Equations (18) and (21) are exactly the same as in the two-dimensional case. Equation (19) is similar, but has an extra term vC_0. The centroid positions will be affected by the cross-wind shear, but, since there is no term involving K_y, not by the cross-wind diffusion. Equation (20) has two extra terms, $2vC_1$ and $2K_yC_0$, showing that the cross-wind dispersion will depend both on the cross-wind shear and on the cross-wind diffusion.

The computations are made by setting up one integrator chain for each moment, each identical with that used in the two-dimensional case. Connexions between the chains,

through potentiometers representing v and K_y, feed the additional terms on the right-hand side of (19) and (20) to the appropriate integrator inputs. This is shown schematically in Figure 15. The connexions between the chains, shown once only in the diagram, have of course to be made at every level of z. Despite the economy of equipment given by the

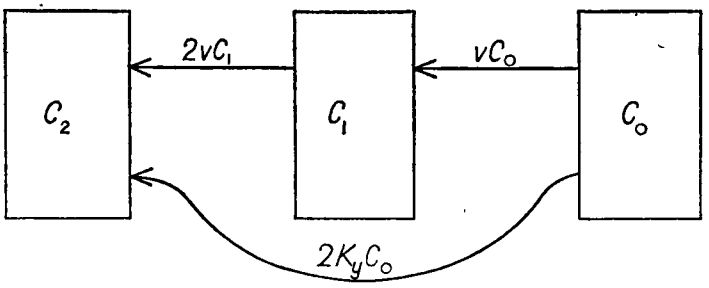

FIGURE 15. Three-dimensional diffusion—schematic computer diagram. The blocks C_0, C_1, C_2 represent three identical integrator chains, one for each moment.

moment method, the number of layers had to be reduced from ten to eight. The cross-wind shear was introduced in such a way as to make the mean cross-wind component $\bar{v}$ through the whole depth of the layer zero. The advantage of this arrangement is that C_1 approaches an asymptotic value, instead of increasing without limit. It does, however, involve negative values of the v coefficients in the bottom half of the model. The desired sign changes are made by inserting inverters in the relevant interchain feeds. Part of the complete circuit diagram is shown in Figure 16.

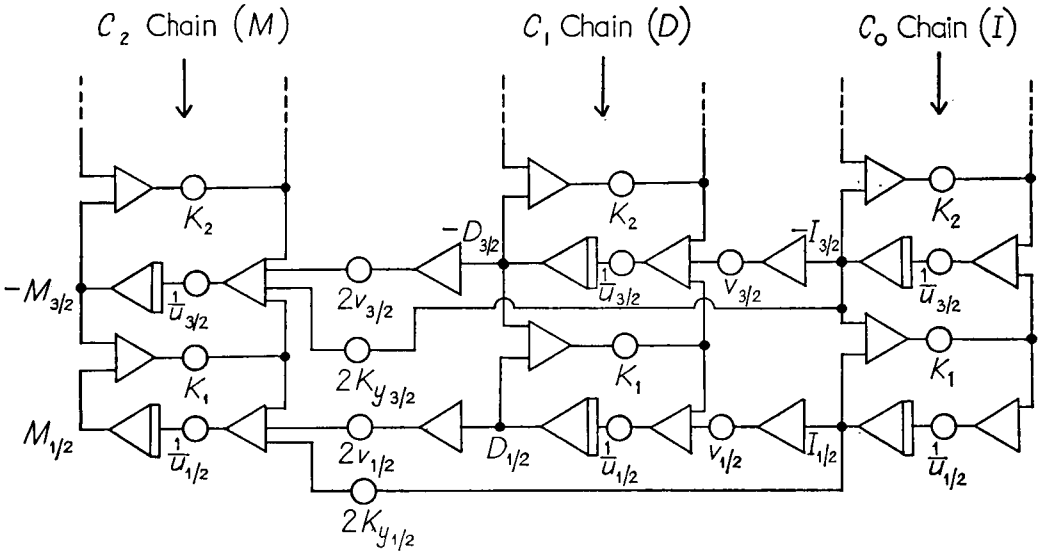

FIGURE 16. Three-dimensional diffusion—bottom two layers of the complete computer diagram (eight layers).

The scaling of the problem proved rather troublesome. As in the two-dimensional problem, the main interest lies in the variation of the parameters. In that case, the dependent variable nowhere exceeded the initial value, and the same applies in this case for

C_0. C_1, however, increases steadily, although as will be seen, it approaches a limiting value at each level if $\bar{v}$ is zero. C_2 also increases steadily, but without limit. The extra inputs to the C_1 and C_2 chains have to be properly related to the existing inputs, and to each other. The method used was again that of normalized variables and normalized parameters. To avoid double subscripts, we write

$$I \equiv C_0 \qquad D \equiv C_1 \qquad M \equiv C_2$$

Subscripts can now be used for the layer number, as before. Using subscript m for maximum values, and primes for computer values, we have

$$I' = \frac{I}{I_m} \qquad \text{etc. for the dependent variables}$$

and

$$K'_z = \frac{K_z}{K_{zm}} \qquad \text{etc. for the parameters.}$$

When dealing with the inter-chain couplings, we write

$$v' = \frac{v}{v_m} \qquad \text{for the feed to the } D \text{ chain}$$

and

$$\left.\begin{aligned} v'' &= \frac{v}{v_r} \\ K'_y &= \frac{K_y}{K_{yr}} \end{aligned}\right\} \qquad \text{for the feeds to the } M \text{ chain.}$$

The notation for the feeds to the M chain is intended to indicate (1) that the 'maximum' (or reference) value for v need not be the same as for the feed to the D chain, and (2) that the reference value K_{yr} (as will be seen) may not be chosen arbitrarily. As before, computer time and downwind distance are related by substituting all the above relations in the finite-difference form of (18), (19) and (20), and comparing coefficients with the corresponding equations for the operation of the computer. The results are as follows:

$$\beta = \frac{K_m(1/u)_m CR}{h^2} \qquad \ldots(22)$$

as before. The computer time constants (CR) of each chain must be equal.

$$Y = \frac{v_m h^2}{K_m} \cdot \frac{D'}{I'} \qquad \ldots(23)$$

Here Y is the cross-wind displacement of the plume-section centroid, D'/I' the ratio of the computer variables, and $v_m h^2/K_m$ the length scale which must be applied to that ratio.

$$\sigma = \frac{v_m h^2}{K_m}\left[\frac{2v_r}{v_m}\left(\frac{M'}{I'}\right) - \left(\frac{D'}{I'}\right)^2\right]^{1/2} \qquad \ldots(24)$$

provided that

$$K_{yr} = \frac{v_m v_r h^2}{K_m} \qquad \ldots(25)$$

Once v_m, v_r, h and K_m are chosen, K_{yr} is fixed by (25). With all the other parameters, having obtained solutions with certain *shapes* of the vertical profiles, they may be given any desired *size*. With K_y, this is not so.

It is interesting to note that it is possible, without going near the computer, to form an idea of the relative contributions of horizontal diffusion and shear to the spread of the cloud. Suppose for simplicity we have $v_m = v_r = v$, $K_m = K_z$, so that the v' and v'' potentiometer settings will be of order one. Then with our eight layers we have from (25) $K_{yr} = v^2H^2/64K_z$. Since $K'_y = K_y/K_{yr}$, a large reference value K_{yr} means a small potentiometer setting K'_y. Let us try a numerical case: $H = 1000$m, $K_y = K_z = 10\text{m}^2/\text{sec}$, $v = 1$ m/sec. Then

$$K'_y = \frac{K_y}{K_{yr}} = \frac{10 \times 10 \times 64}{1 \times 10^6} = 0{\cdot}0064.$$

It is clear that whatever the precise values of D' and I', of the two inputs to the M' integrator, the $1 \times D'$ term will greatly outweigh the $0{\cdot}0064 \times I'$ term. It is already possible to say from equation (25) that the requirements for the shear effect to dominate are: a large shear, a deep layer, small vertical diffusion, or some combination of these; and that these demands will often be met in practice. In scaling the problem for the analogue, almost as a matter of course an assessment was made of the relative magnitudes of the terms involved. In fact a dimensional analysis of the problem was performed, and this analysis could no doubt be purged of its computer trappings and made to stand on its own feet as a calculation to show the order of magnitude of the wind shear effect. Moreover, as an unsought bonus, we have been presented with the dimensionless variables to use:

$$\frac{K_z}{uH^2}x, \qquad \frac{K_z}{vH^2}y, \qquad \frac{1}{H}z.$$

It will often be found that the process of scaling for the analogue computer, although tiresome in detail, gives more physical insight than a direct attack by numerical methods.

Returning to the details of the scaling, it will be noted that the length-scale for σ in front of the square brackets in (24) is the same as that for Y in (23). A numerical factor $2v_r/v_m$ appears inside the brackets. The simplest course is to make this unity by having $v_m = 2v_r$. The v-potentiometer settings to the M chain are then twice those to the D chain, which agrees in a natural way with the factor 2 in the $2vD + 2K_yI$ terms. This was done in the early work, but it is not always satisfactory, as a v_m value which produces full-scale D' values, may drive M' off scale. It was found best at first to seek suitable values of v_m and v_r at the computer console. All the M-feeds were disconnected, and maximum v' values for the chosen profile shapes set up. A trial run was then made, and the behaviour of the D' values watched. If they increased too rapidly, all the v' values were reduced in a suitable proportion. Then the v'' settings to the M' chain were reconnected, and another trial run made to observe M'. It was found that suitable values of $2v_r/v_m$ ranged from 2 for short solution times, to 32 for the longest times. After a little experience had been gained of the form of the solutions, it was not too difficult to choose v' and v'' values that

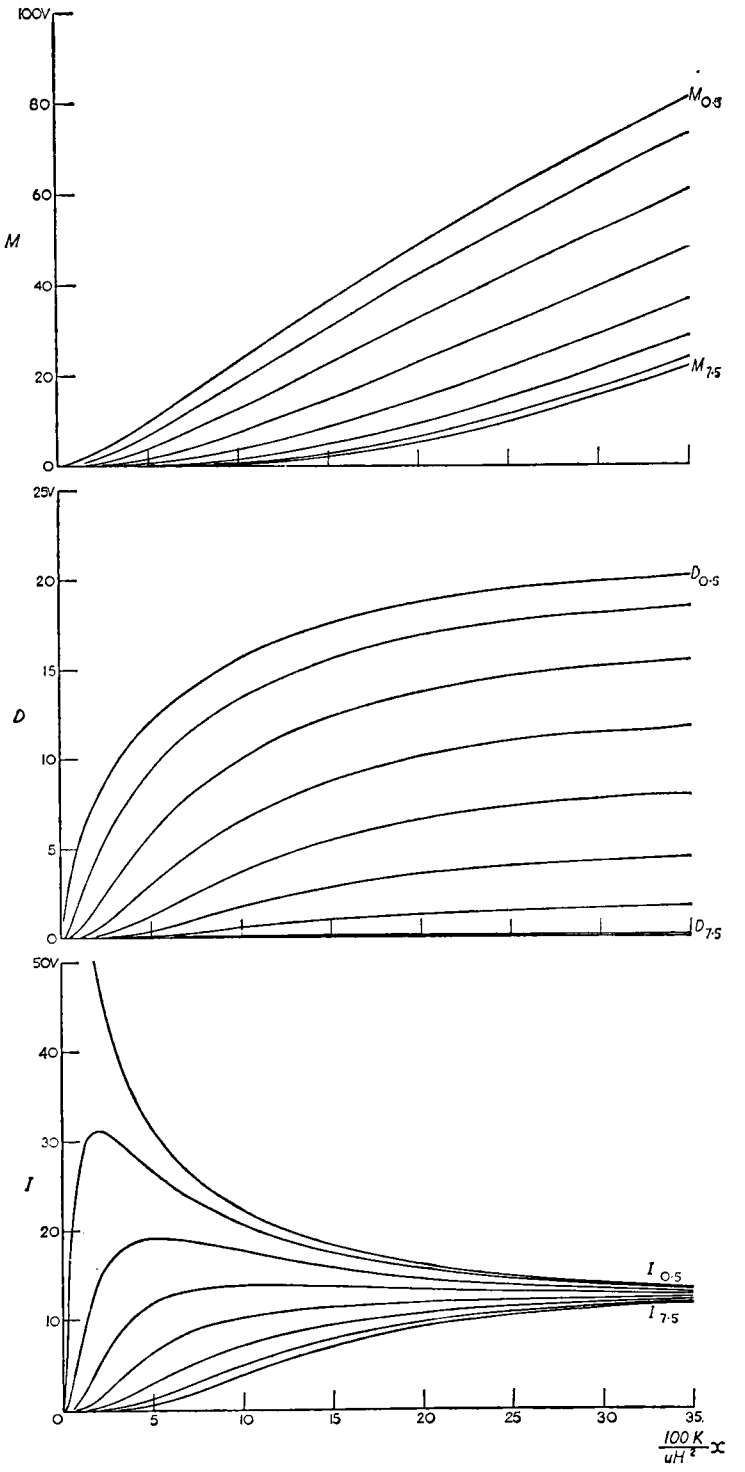

FIGURE 17. Three-dimensional diffusion. u = const., K_z = const., $K_y = 0$. Linear cross-wind shear as in Figure 15. The three moments as functions of downwind distance x. The units on the vertical scales are computer voltages in each case. Subscripts to I, D and M relate to the layers of the eight-layer model.

would give useful output voltages at the first attempt. Figure 17 shows sets of I', D' and M' curves for the case K_z = constant, $K_y = 0$, u = constant, shear in v as in Figure 15, and source at the ground. The I' curves are similar to those obtained in the two-dimensional case, and all tend to an asymptotic value of 1/8 of full-scale, corresponding to equal total concentration in each layer. The D' curves increase at first and then level off, to a different asymptotic value at each height. D' at the top layer is zero throughout, since in this case the negative cross-wind displacement in the bottom half of the model is exactly balanced by the positive displacement above. The plume displacements Y and the standard deviations σ are now calculated according to (23) and (24). Three methods have been used to do this. First, the three moments may be recorded with the two-co-ordinate plotter. This is rather a slow process as a separate run has to be made for each of the 24 curves. The values are read off at convenient intervals, and Y and σ calculated by hand. The major part of the results so far has been obtained in this way. Secondly, when the graphical method had given some idea of the form of the results, the computation was stopped manually at the chosen times, and all the outputs read on the digital voltmeter. This procedure was especially useful for investigating the later stages of the computations, when the variables were changing only slowly, and graphical recording was most time-consuming. The major part of the results has been obtained by this method. This proved on the whole to be the most satisfactory way, because the graphical recording method cannot take advantage of the full accuracy of the computer. In the early part of the computation, $2v_rM'/v_mI'$ and $(D'/I')^2$ are nearly equal, and the smallness of their difference results in a rather poor determination of σ^2. On the other hand, the digital method means stopping the computation for a matter of minutes to read the integrator output, and is therefore only feasible on a computer with very low drift. A third method, on which a good deal of effort was expended, was to compute Y and σ directly on the machine, using servo-multipliers for division, squaring and square rooting. The analogue machine is not really suitable for repeated algebraic operations. The quality of the non-linear elements is much below that of the linear equipment, as regards both accuracy and noise. In conventional applications, non-linear operations are usually followed by an integration, which smoothes out the noise. In our case, it tended to be cumulative. Great care had to be taken to fill the full scale of the dependent variables, and even then the outputs were very shaky. It seems that the best results would be obtained on a machine having automatic digital output, so that the final processing of the moments could be done on a digital machine.

Figure 18 shows the values of the plume displacements Y, and the standard deviations σ, as functions of downwind distance, calculated from the moments of Figure 17 by the equations (23) and (24). The graphs are actually composites prepared from a number of solutions in which the coefficients were adjusted to obtain maximum accuracy over overlapping ranges of downwind distance. To avoid confusion in the diagram, values are not shown for all of the eight layers. It will be seen that the Ys ultimately reach steady values at all levels, but decreasing with height to zero at the top. This indicates that a balance has been reached between horizontal shear and vertical diffusion. The σ values vary little with height, but increase slightly from the ground to a maximum near the middle of the layer, and then fall again to an intermediate value at the top. σ varies linearly with x over a wide range, but eventually approaches an asymptotic rate of expansion with $\sigma^2 = 2K_vt$, where K_v may be thought of as a virtual diffusion coefficient due to shear. Saffman[11] predicts the asymptotic form of these results, and the numerical coefficients for this particular case are given by Tyldesley and Wallington[12], using Laplace transform methods. A horizontal

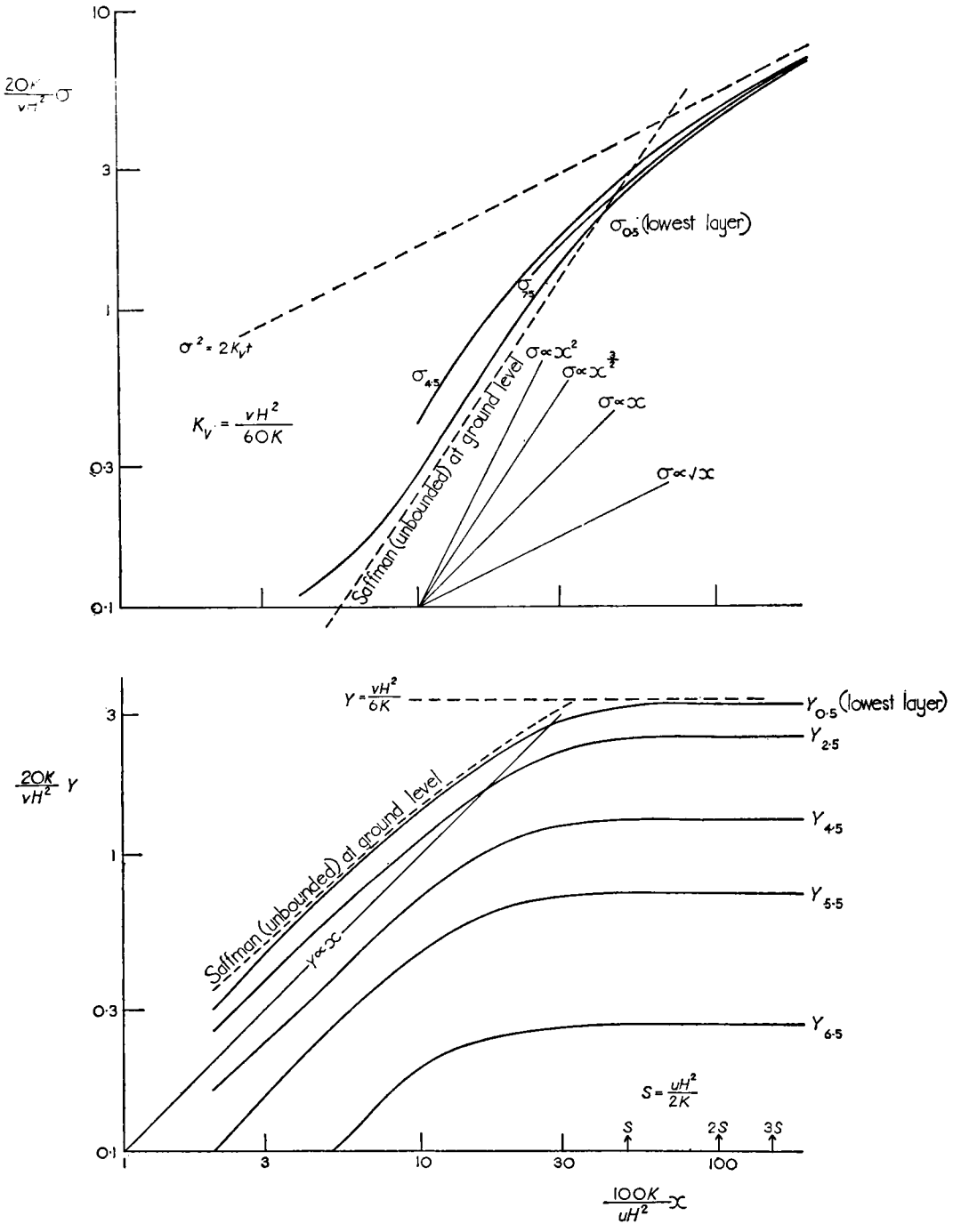

FIGURE 18. Three-dimensional diffusion. u = const., K_z = const., $K_y = 0$. Standard deviations (σ, above) and displacements of the plume centroids (Y, below) of the plume sections, as a function of the downwind distance x. Subscripts to σ and Y relate to the layers of the eight-layer model.

line on the Y graph corresponds to the analytical asymptotic value for the bottom layer of $(\Delta v H^2)/(6K)$. An inclined line on the σ graph corresponds to the analytical asymptotic rate of expansion $\sigma^2 = 2K_v x/u$. The computed line attains the correct slope, although it yields values about 3 per cent less than the analytical formula. For the early part of the solution when the upper lid has no influence, comparison of the analogue results for the bottom layer can be made with Saffman's solution for an unbounded atmosphere. These also are plotted as broken lines in Figure 18. It can be seen that the computer solutions for Y and σ in the lowest layer are within 2 per cent agreement with the analytical deductions for ground level for a range of distance given by $0{\cdot}05 < (Kx)/(uH^2) < 0{\cdot}2$. For lesser distances errors mainly due to the finite difference approximations become significant.

These numerical comparisons show that despite the reduction of layers from ten to eight, the greater complexity of the three-dimensional circuit, and the processing to which the moments are subjected, the accuracy is still ample for practical purposes at both long and short ranges. This gives confidence in the use of the analogue model at intermediate ranges, and for forms of the parameters which cannot be attacked analytically.

Downwind distances S, $2S$, and $3S$ where $S = (uH^2)/(2K)$ are marked on the x-axis of Figure 18. When $x = S$, the variation of total concentration with height is less than 10 per cent (i.e. would be considered substantially constant under experimental conditions) but the increase of σ with x is still approximately linear, and the asymptotic rate of expansion is not attained until about $x = 3S$. Thus the analogue results are a useful supplement to the analytical information, even on asymptotic values, because they show in what range they can properly be applied.

If it is desired to obtain actual concentration values, it is necessary, short of computing moments higher than the second, to assume a Gaussian distribution. Use can be made of the fact that the peak concentration is given by $1/\sqrt{2\pi}\cdot I/\sigma$, to find the concentrations at various distances in the cross-wind direction from tables of the normal curve. Then all the material necessary is available to construct sections in the (yz) plane at any downwind distance x. The centroid at each level is marked out at distance Y, and from the centroid the σ, 2σ and 3σ points are measured on each side. Finally the concentrations are inserted using the I/σ values and the normal curve table. Isopleths may then be drawn, bearing in mind that with the no-flux boundary condition, they must be normal to the upper and lower boundaries. A series of sections prepared in this way is shown in Figure 19.

The concentration values will normally be calculated at first in terms of the computer variables, I' and

$$\sigma' = \left[\frac{2v_r}{v_m}\,\frac{M'}{I'} - \left(\frac{D'}{I'}\right)^2\right]^{1/2}.$$

To convert to absolute values in terms of the source strength, the continuity condition is again used, and the result is that the proper label for a concentration calculated in the way described above is given by

$$\frac{1}{\sqrt{2\pi}}\,\frac{I'}{\sigma'} = \frac{u_s v_m H^3}{n^3 K_m Q}\chi_{\text{peak}}$$

where u_s is u at the source level.

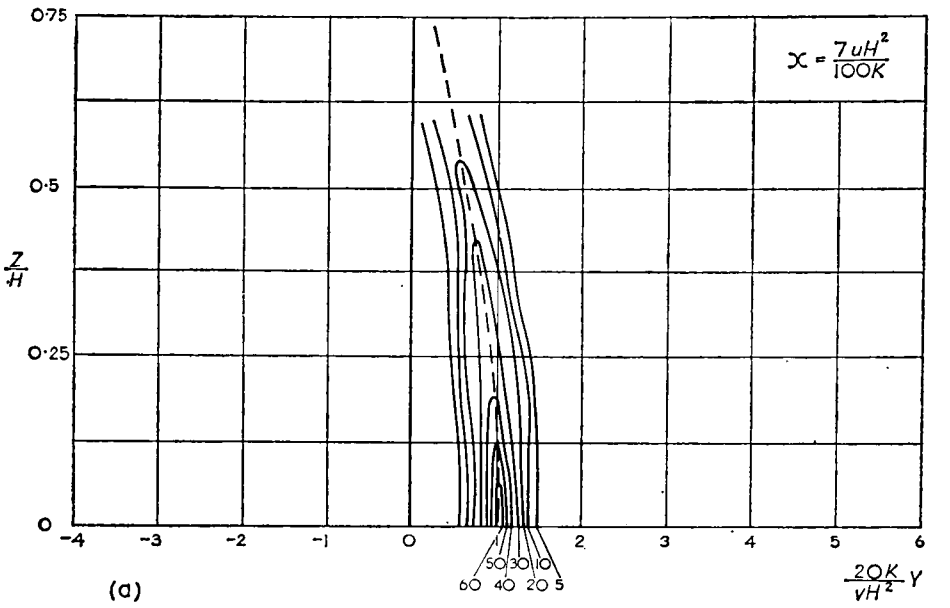

FIGURE 19. Three-dimensional diffusion. Figures (*a*) to (*e*) are sections in the [*yz*] plane at different downwind distances *x*. Prepared from the curves of Figure 18. Concentrations are in units of $(128K)/(uH^3)Q$.

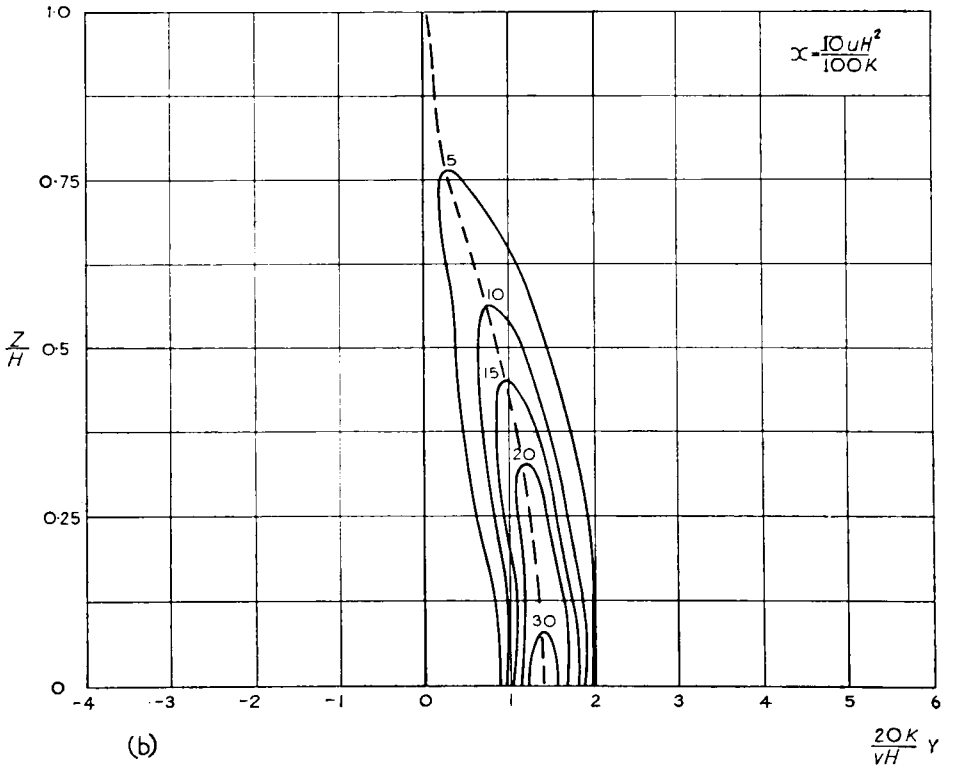

FIGURE 19. *continued.*

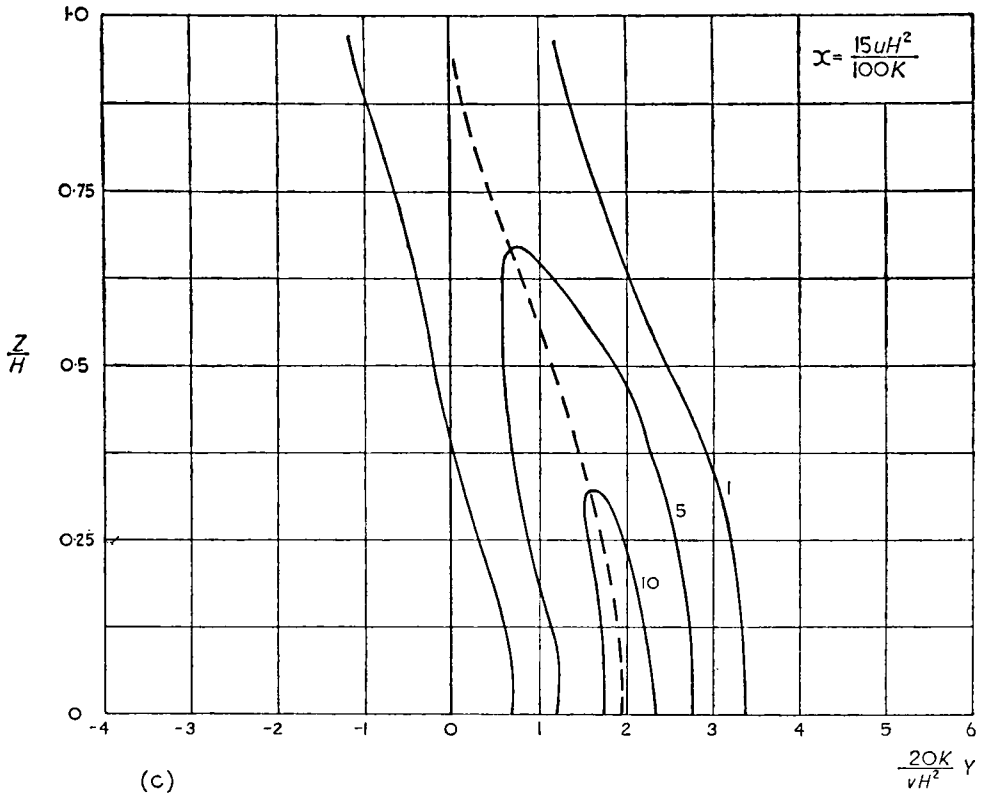

FIGURE 19. *continued.*

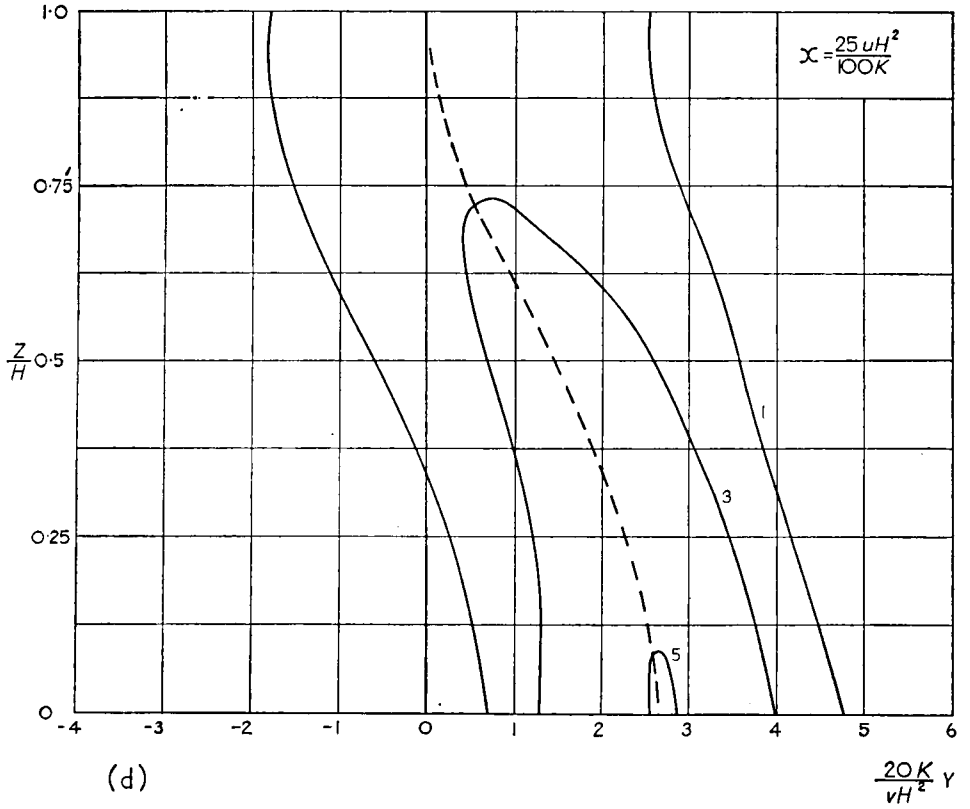

FIGURE 19. *continued.*

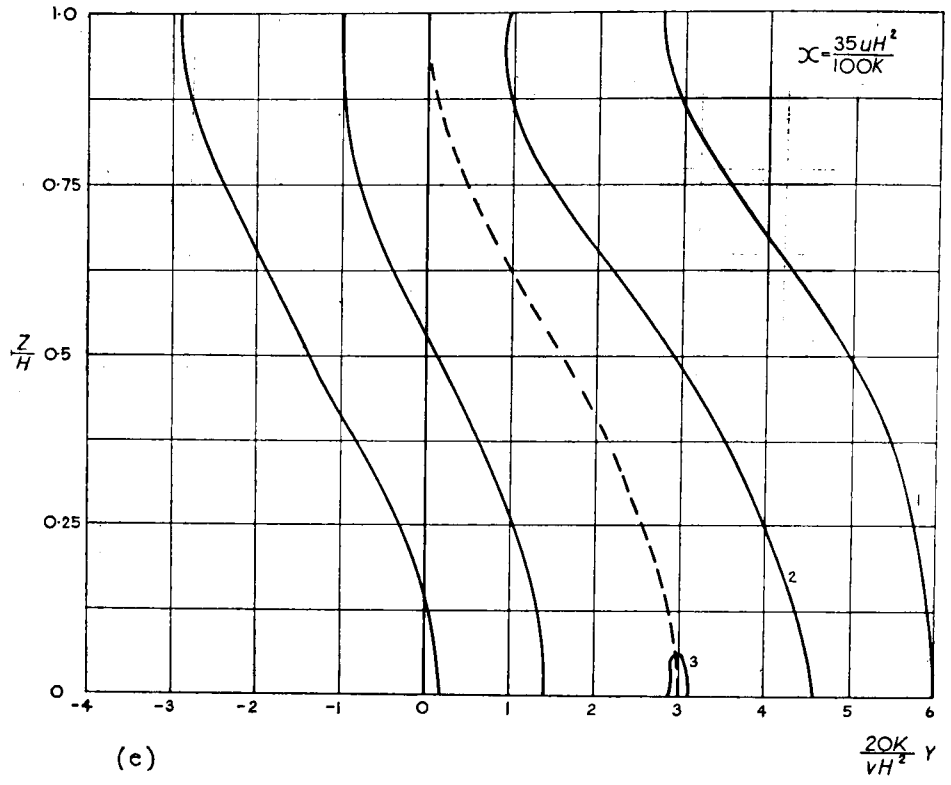

FIGURE 19. *continued.*

APPLICATION OF COMPUTER—INSTANTANEOUS LINE SOURCE

The equation in this case is

$$\frac{\partial \chi}{\partial t} + u\frac{\partial \chi}{\partial x} = \frac{\partial}{\partial z}\left(K_z \frac{\partial \chi}{\partial z}\right) + K_x \frac{\partial^2 \chi}{\partial x^2} \qquad \ldots(26)$$

with the conservation condition

$$Q = \int_0^\infty \int_{-\infty}^\infty \chi \, dx \, dz \qquad \ldots(27)$$

where Q is now the amount of material emitted per unit length of the cross-wind line.

As before, we take finite differences in z. We have to decide whether to take moments in x or t. The decisive factor is that while it is reasonable to treat the horizontal space-distributions as symmetrical and Gaussian, time distributions are often asymmetrical; for the cloud may expand significantly while passing the fixed sampling point.

Moments are therefore taken in x, taking t as the continuous variable. This leads to instantaneous cross-sections of the cloud in the (x, z) plane. If time sequences at fixed x are required, they have to be found in a more round-about way. Fortunately the (x, z)

sections are easily obtained. If we take equations (13) and (14) for the continuous point source, and make the substitutions:

$$\begin{aligned} x &\rightarrow t \\ y &\rightarrow x \\ u &\rightarrow 1 \\ v &\rightarrow u \end{aligned} \qquad \ldots(28)$$

we obtain equations (26) and (27) for the instantaneous line source. It follows that every solution for the continuous point source, with u constant, may be interpreted as a solution for the instantaneous line source. All that is necessary is to apply the transformation (28) to the scaling equations (22), (23), (24) and (25).

It will be remembered that in the continuous source case, the mean cross-wind component $\bar{v}$ through the whole layer is zero. In the instantaneous source case, this corresponds to the alongwind component u, which will normally have the same sign at all heights. To retain the advantages of balanced shear, it is necessary to use axes moving with the cloud at speed $\bar{u}$, which may conveniently be the mean speed in the whole layer. Then in labelling the x-axis of a section at a time $t = t_1$, it must be remembered that its origin is displaced to the right by an amount $\bar{u}t_1$, relative to the origin fixed on the ground. On a sequence of time cross-sections, the vertical line corresponding to a fixed sampling distance $x = x_1$, will first intersect the cloud on the right, move steadily through it on successive sections, and finally emerge from the left on the last section. The concentrations may be read off at each intersection, and transferred to a (z, t) section if desired. It will be seen that a whole family of (x, z) sections is required to produce one (z, t) section. Also, the times of the (x, z) sections must be carefully chosen in relation to the shear u and mean wind $\bar{u}$. Otherwise, the cloud may be intersected on only one or two (x, z) sections, or it may be intersected on each section, but not fully traversed. A (z, t) section constructed in this way, with parameter values designed to bring out the asymmetry, is given in Figure 20.

APPLICATION OF COMPUTER—INSTANTANEOUS POINT SOURCE

The methods described so far make it possible to calculate concentrations as functions of z, and any two of (x, y, t). In the instantaneous point source problem all three are involved. Using t as the continuous variable, moments in both x and y are needed. We define

$$C_{nm} = \int_{-\infty}^{\infty} \chi\, x^n\, y^m \, \mathrm{d}x\, \mathrm{d}y \qquad \ldots(29)$$

The diffusion equation is

$$\frac{\partial \chi}{\partial t} + u\frac{\partial \chi}{\partial x} + v\frac{\partial \chi}{\partial y} = \frac{\partial}{\partial z}\left(K_z \frac{\partial \chi}{\partial z}\right) + K_y \frac{\partial^2 \chi}{\partial y^2} + K_x \frac{\partial^2 \chi}{\partial x^2} \qquad \ldots(30)$$

with the conservation condition

$$Q = \int_0^{\infty}\int_{-\infty}^{\infty}\int_{-\infty}^{\infty} \chi \, \mathrm{d}x\, \mathrm{d}y\, \mathrm{d}z \qquad \ldots(31)$$

where Q is now the total amount of material emitted.

The differential equations for the moments are

$$\frac{\partial C_{00}}{\partial t} = \frac{\partial}{\partial z}\left(K_z \frac{\partial C_{00}}{\partial z}\right) \quad \ldots(32)$$

$$\frac{\partial C_{10}}{\partial t} = \frac{\partial}{\partial z}\left(K_z \frac{\partial C_{10}}{\partial z}\right) + uC_{00} \quad \ldots(33)$$

$$\frac{\partial C_{01}}{\partial t} = \frac{\partial}{\partial z}\left(K_z \frac{\partial C_{01}}{\partial z}\right) + vC_{00} \quad \ldots(34)$$

$$\frac{\partial C_{20}}{\partial t} = \frac{\partial}{\partial z}\left(K_z \frac{\partial C_{20}}{\partial z}\right) + 2uC_{10} + 2K_xC_{00} \quad \ldots(35)$$

$$\frac{\partial C_{02}}{\partial t} = \frac{\partial}{\partial z}\left(K_z \frac{\partial C_{02}}{\partial z}\right) + 2vC_{01} + 2K_yC_{00} \quad \ldots(36)$$

and the conservation condition becomes

$$Q = \int_0^\infty C_{00}\,dz \quad \ldots(37)$$

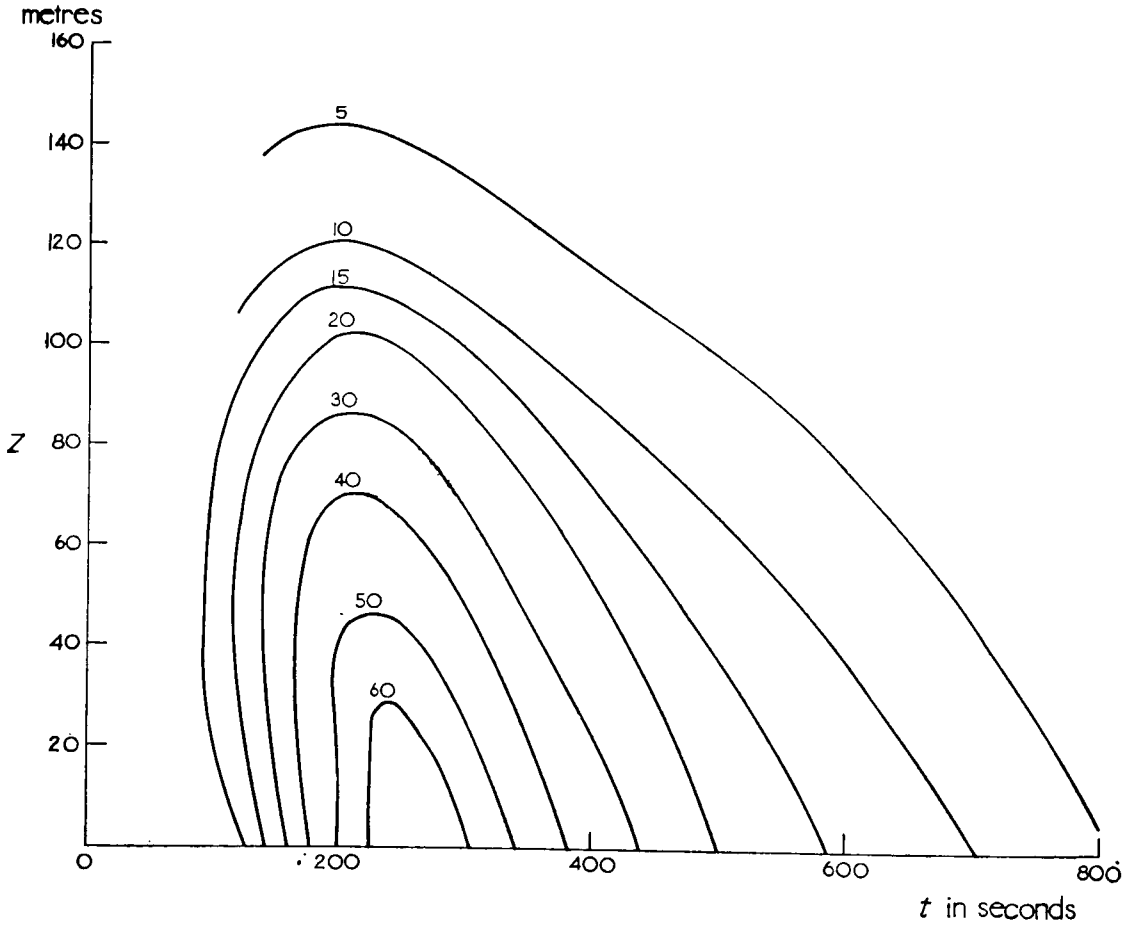

FIGURE 20. Instantaneous line source: time cross-section at fixed sampling distance. X = 600 m, K_z = 10 m^2s^{-1}, K_y = (100/64) m^2s^{-1}, $\bar{u}$ = 5m s^{-1}, u = 10m s^{-1}, H = 160 m. Concentration values in units of Q/16,000 m.k.s.

The equations for the x-moments are independent of the y variables and parameters, and conversely, so that X, Y, σ_x and σ_y can be completed exactly as before. With an assumed Gaussian distribution in x and y, the concentration isopleths in the (x, y) plane will be ellipses, and it seems at first that a diagram can be laid out in the x–y plane as in Figure 21 and the isopleths drawn in at once (solid line). Unfortunately, an infinity of ellipses can be drawn through four points (another is shown by the broken line in Figure 21) and the

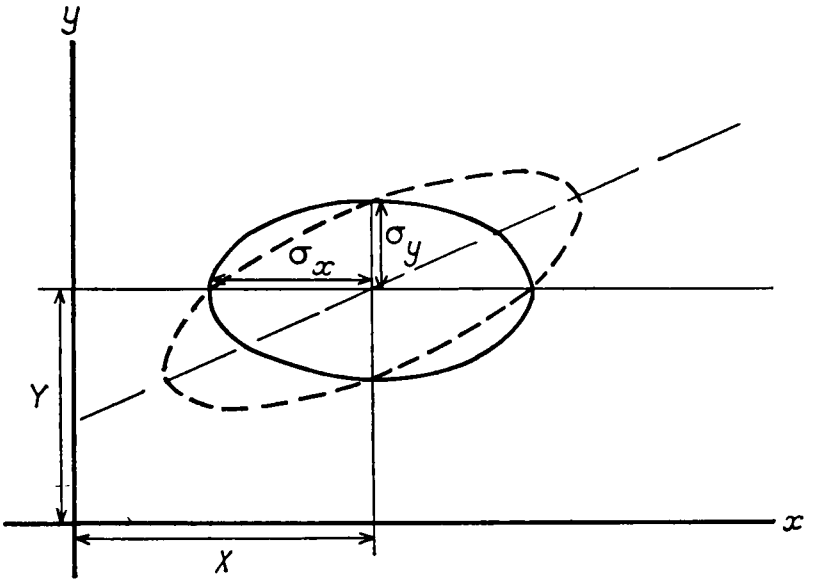

FIGURE 21. Instantaneous point source, showing the ambiguity in drawing concentration isopleths when only X, Y, σ_x, σ_y, are given.

axes of the ellipse must be determined. To do this we need the cross-moment the equation for which is

$$\frac{\partial C_{11}}{\partial t} = \frac{\partial}{\partial z}\left(K_z \frac{\partial C_{11}}{\partial z}\right) + vC_{10} + uC_{01} \qquad \ldots(38)$$

The angle θ between the axes of the ellipse and the co-ordinate axes is given by

$$\tan 2\theta = \frac{2C_{11}}{\sigma_x^2 - \sigma_y^2} \qquad \ldots(39)$$

Because of the second and third terms on the right-hand side of equation (38) cross-coupling between the variables x and y cannot be avoided. Figure 22 indicates schematically, in the same way as Figure 14 for the continuous source, the necessary integrator chains and their interconnexions, to solve the problem. The demand on equipment is not as bad as it looks, because the problem can be split up. X and σ_x require only three integrator chains, for C_{00}, C_{10} and C_{20}, as before; and the same equipment may be used again to find Y and σ_y. However C_{11} requires simultaneously the four chains for C_{00}, C_{10}, C_{01} and C_{11}. To compute C_{11} would require either a further reduction in the number of layers, or a larger machine. Fortunately, the concentration pattern can be found without this, if the shear is in u only or v only. For if $v = 0$, $C_{01} = 0$ from equation (34) and therefore the

last two items on the right-hand side of (38) vanish. Then C_{11} is always zero, and the axes of the concentration ellipses are parallel to the co-ordinate axes. It seems likely that enough information to indicate the solution of practical problems could be obtained in this way.

CONCLUSION

The applications of the computing methods described in this paper are likely to follow two lines. On the one hand, wherever the parameters u can be measured and K estimated from atmospheric measurements, comparison with observed concentrations will throw light on the value of the theory of turbulence underlying the estimate. This application is likely to be mostly two-dimensional, because of the difficulty of adequate three-dimensional sampling. On the other hand, the sampling difficulty will not inhibit theoretical study of the three-dimensional cases. Here the analogue computer may be regarded as a convenient laboratory simulator of experiments which it is difficult or impossible to carry out in the atmosphere.

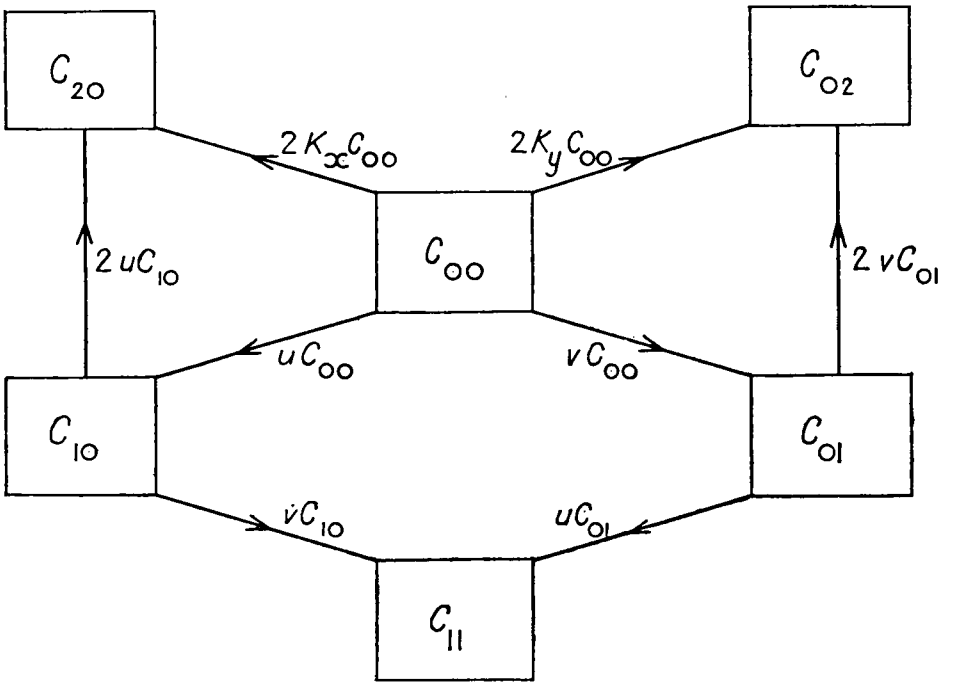

FIGURE 22. Instantanieous point source: schematic computer diagram. Each block represents an integrator chain for one of the moments, and the terms represented by the interconnexions are shown by each arrow.

CHOICE OF ANALOGUE OR DIGITAL METHODS OF COMPUTING

It is thought that a few remarks on this subject may be of use, particularly as it is one which arouses strong partisan feelings. In the case of this atmospheric diffusion work, it is probably easier than usual to form a balanced view, because a programme for a digital computer (Ferranti Mercury) was developed by Mr. C. E. Wallington, in parallel with the

analogue method. This model had thirty layers for both two and three-dimensional diffusion. Although it has been shown that satisfactory results can be obtained with only eight or ten layers, the larger number is more convenient, as it is less essential to ensure that the solution uses all the available layers. Also, in the three-dimensional case, the digital computer processes the moments before print-out, to produce concentrations, centroid displacements and standard deviations directly. Although the analogue machine, with its parallel operation, can produce the moments more quickly than the digital can, the tedious hand-processing of the analogue results gives the digital machine an advantage in overall speed. One advantage of the analogue machine is that it is always stable for parabolic equations. This is not the case for the digital machine. For stability, the steps in the x and z dimensions must be properly related, and this relation is not unique but must be empirically determined, the relation varying also with the parameter values. Consequently, it was of great assistance in the development of the digital programme to have reliable values obtained by the analogue method, to test the stability of the results. Mention has already been made on page 23 of the general insight based on dimensional analysis, gained in the course of scaling the problem for the analogue machine.

For large problems, an analogue machine, because of its mode of parallel operation, must have much equipment, although if the equipment is available, the solution time may be no longer than for a small problem. A digital machine uses much time, utilizing the same equipment, so that its capacity is never over-run in the same absolute way as may occur with an analogue machine.

The general conclusion is that the two types of machine are complementary. For the exploratory stages of a problem, particularly if not fully formulated or where there is an intuitive element in the approach, the analogue machine has great advantages. For large volumes of production work, for large problems, and in cases where the highest accuracy is required, the digital machine is likely to be best.

ACKNOWLEDGEMENTS

The author is indebted to C. E. Wallington for suggesting the moment idea which is fundamental to the three-dimensional treatment. The analogue computing was carried out at the Royal Armament Research and Development Establishment, Fort Halstead. The staff there, particularly B. J. Rolls, gave much help with the programming and running of the problems. N. Thompson obtained the concentration profiles given in Figures 19(*a*) to (*e*), and the profiles computed with the *RC* network in the same figures.

BIBLIOGRAPHY

1. SUTTON, O. G.; Micrometeorology. New York, McGraw-Hill Book Co. Inc., 1963, Chapters 4 and 8.
2. SMITH, F. B.; Convection-diffusion processes below a stable layer. Unpublished government report, 1957.
3. SMITH, F. B.; Convection-diffusion processes below a stable layer, Part II. Unpublished government report, 1957.
4. PASQUILL, F.; Some observed properties of medium-scale diffusion in the atmosphere. *Quart. J. R. met. Soc., London*, **88**, 1962, p. 70.
5. PASQUILL, F.; The determination of eddy diffusion from measurements of turbulent energy. *Quart. J. R. met. Soc., London*, **89**, 1963, p. 95.

6. JONES, J. I. P. and BUTLER, H. E.; The measurement of gustiness in the first few thousand feet of the atmosphere. *Quart. J. R. met. Soc., London*, **84**, 1958, p. 17.
7. THOMPSON, N.; Short-range vertical diffusion in stable conditions. *Quart. J. R. met. Soc., London*, **91**, 1965, p. 175.
8. KARPLUS, W. J. and SOROKA, W. W.; Analog methods. New York, McGraw-Hill Book Co. Inc., 1959.
9. JACKSON, A. S.; Analog computation. New York, McGraw-Hill Book Co. Inc., 1959.
10. BROCK, F. V.; Analog computing techniques applied to atmospheric diffusion: Continuous line source. *J. app. Met.*, **1**, 1962, p. 444.
11. SAFFMAN, P. G.; The effect of wind shear on horizontal spread from an instantaneous ground source. *Quart. J. R. met. Soc., London*, **88**, 1962, p. 382.
12. TYLDESLEY, J. B. and WALLINGTON, C. E.; The effect of wind shear and vertical diffusion on horizontal dispersion. *Quart. J. R. met. Soc., London*, **91**, 1965, p. 158.

Printed in England for Her Majesty's Stationery Office by J. W. Arrowsmith Ltd., Bristol
Dd. 120358 K7 10/65

© *Crown copyright 1965*

Published by
HER MAJESTY'S STATIONERY OFFICE

To be purchased from
49 High Holborn, London W.C.1
423 Oxford Street, London W.1
13A Castle Street, Edinburgh 2
109 St. Mary Street, Cardiff
39 King Street, Manchester 2
50 Fairfax Street, Bristol 1
35 Smallbrook, Ringway, Birmingham 5
80 Chichester Street, Belfast 1
or through any bookseller

S.O. Code No. 40-164-22